

# Hypersphere Secure Sketch Revisited: Probabilistic Linear Regression Attack on IronMask in Multiple Usage

Pengxu Zhu  
Shanghai Jiao Tong University  
Shanghai, China  
zhupengxu@sjtu.edu.com

Lei Wang\*  
Shanghai Jiao Tong University  
Shanghai, China  
wanglei\_hb@sjtu.edu.cn

## ABSTRACT

Protection of biometric templates is a critical and urgent area of focus. **IronMask** demonstrates outstanding recognition performance while protecting facial templates against existing known attacks. In high-level, **IronMask** can be conceptualized as a fuzzy commitment scheme building on the hypersphere directly. We devise an attack on **IronMask** targeting on the security notion of renewability. Our attack, termed as **Probabilistic Linear Regression Attack**, utilizes the linearity of underlying used error correcting code. This attack is the first algorithm to successfully recover the original template when getting multiple protected templates in acceptable time and requirement of storage. We implement experiments on **IronMask** applied to protect **ArcFace** that well verify the validity of our attacks. Furthermore, we carry out experiments in noisy environments and confirm that our attacks are still applicable. Finally, we put forward two strategies to mitigate this type of attacks.

## CCS CONCEPTS

• Security and privacy → Privacy protections; Cryptanalysis and other attacks.

## KEYWORDS

biometric template protection, face recognition, secure sketch, fuzzy commitment, security analysis

## ACM Reference Format:

Pengxu Zhu and Lei Wang. YYYY. Hypersphere Secure Sketch Revisited: Probabilistic Linear Regression Attack on IronMask in Multiple Usage. In *Proceedings of Make sure to enter the correct conference title from your rights confirmation email (Conference acronym 'XX)*. ACM, New York, NY, USA, 14 pages. <https://doi.org/XXXXXXX.XXXXXXX>

## 1 INTRODUCTION

Biometric-based authentication has been under intensive and continuous investigation for decades. Recent works use deep neural networks to extract discriminative features from users' biometrics and achieve significant advances, such as facial images. **ArcFace**[11], which is one of the state-of-the-art face recognition system, projects

the face images to templates on a hypersphere and utilizes angular distance to distinguish identities.

However, the exposure of facial templates has the potential to cause severe threats to both user privacy and the entire authentication system. There have been a great number of attacks to show the risky leakage of templates and some even can reconstruct the biometric images from corresponding templates, including face [29, 33, 34], fingerprint [7], iris [14] and finger vein [23]. Therefore, the biometric template protection (BTP) technique is becoming pressing due to the security risks arising from widespread biometric-based authentication system.

BTP technique primarily achieves three goals: *irreversibility*, *renewability* and *unlinkability* with considerable recognition performance. Irreversibility prevents the reconstruction of the original biometric templates, ensuring the security of the biometric template for one-time use. Renewability ensures the irreversibility with newly issued protected biometric template even though old ones have been leaked, enabling its multiple usage. Unlinkability guarantees that the protected biometric templates from the same person cannot be associated with a single identity. The unlinkability is the most robust property and considerably more challenging to achieve, compared to the irreversibility and the renewability.

The fuzzy-based scheme is a promising technique to implement BTP. Fuzzy-based schemes include fuzzy extractor [12], fuzzy vault [20] and fuzzy commitment [21]. They commonly consist of two functions: *information reconciliation* and *privacy amplification*. Information reconciliation maps similar readings to an identical value, while privacy amplification converts the value to an uniformly random secret string. Information reconciliation is frequently implemented by secure sketch based on an error-correcting code (ECC). Privacy amplification is accomplished by extractors or cryptographic hash function. The fuzzy-based scheme has been used to protect biometric templates in the binary space or set spaces with error-correcting codes [3, 27] and real-valued space  $\mathbb{R}^n$  with lattice code [18, 22]. Nonetheless, there have no fuzzy-based scheme on hypersphere without directly transforming to the binary space until the first result in [24]. Kim et al. devise an error correcting code on hypersphere to build a secure sketch and in turn a fuzzy commitment scheme, named **IronMask**. They apply **IronMask** to protect facial template on **ArcFace** with template dimension as  $n = 512$ , recommending the error correcting parameter  $\alpha = 16$ . The combination achieves a true accept rate(TAR) of 99.79% at a false accept rate(FAR) of 0.0005% and providing at least 115-bit security against known attacks. They claimed that their scheme satisfies irreversibility, renewability and unlinkability. To the best of our knowledge, it's the best BTP scheme to provide high security while preserving facial recognition performance without other secrets.

\*Corresponding author.

Permission to make digital or hard copies of all or part of this work for personal or classroom use is granted without fee provided that copies are not made or distributed for profit or commercial advantage and that copies bear this notice and the full citation on the first page. Copyrights for components of this work owned by others than the author(s) must be honored. Abstracting with credit is permitted. To copy otherwise, or republish, to post on servers or to redistribute to lists, requires prior specific permission and/or a fee. Request permissions from [permissions@acm.org](mailto:permissions@acm.org).

Conference acronym 'XX, XXXX, XXXX

© 2024 Copyright held by the owner/author(s). Publication rights licensed to ACM. <https://doi.org/XXXXXXX.XXXXXXX>

## 1.1 Our Contributions.

We analyze the renewability and the unlinkability of **IronMask**. With multiple protected templates, we devise an attack, named as **probabilistic linear regression attack**, that can successfully recover the original face template. Let  $n$  denote the dimension of the output template and  $\alpha$  denote the error correcting parameter. The algorithm's complexity is  $O(n^p e^{c\alpha})$  where  $p$  is relative to the underlying used linear regression solver algorithm and  $c$  is relative to how many protected templates obtained. We apply the probabilistic linear regression attack on **IronMask** protecting **ArcFace** with  $n = 512$  and  $\alpha = 16$ . The experiment is carried out on a single laptop with Intel Core i7-12700H running at 2.30 GHz and 64 GB RAM. The experimental results show that the execution time is around 5.3 days when obtaining  $n - 1 = 511$  protected templates, and is around 621 days when obtaining only 2 protected templates for SVD-based linear solver. As for LSA-based linear solver, the execution time is around 4.8 days when obtaining 3 protected templates and around 7.1 days when obtaining 281 protected templates. We note that the attack algorithm is fully parallelizable, and hence using  $m$  machines leads to a linear speedup of  $m$  times. Moreover, we carry out experiments in noisy scenarios and demonstrate that our attacks are still applicable, substantiating its practical effectiveness in the real world. Furthermore, we propose two plausible defence strategies: Add Extra Noise in Sketching Step and Salting on strengthening **IronMask** in order to mitigate our attacks and reach around 63-bit security.

## 2 RELATED WORKS

### 2.1 Face Recognition on Hypersphere

Face recognition employing deep neural networks typically involves two sequential stages. Firstly, the face image is ingested as input, and an embedded facial representation, serving as a template, is generated as output; Secondly, the similarity score between two face templates is computed, enabling the determination of whether two face images correspond to the same individual.

Recent works have discovered that instead of using contrastive loss [9] and triplet loss [41], angular margin-based losses exhibits superior performance in training on large-scale dataset, such as SphereFace [28], **ArcFace** [11] and MagFace [30]. Under these face recognition frameworks, the face templates are constraint on a unit-hypersphere and the similarity score of two templates  $\mathbf{w}_1, \mathbf{w}_2$  is calculated as cosine similarity  $\text{Score}(\mathbf{w}_1, \mathbf{w}_2) = \arccos \frac{\mathbf{w}_1 \cdot \mathbf{w}_2}{|\mathbf{w}_1| |\mathbf{w}_2|}$ .

### 2.2 Fuzzy-based BTP on Face Recognition

For neural network based face recognition systems, many protection techniques based on error-correcting code or secure sketch have been proposed. [35, 43] directly learn the mapping from face image to binary code, while [1, 31] transform the face template from real-value to binary code by recording other information. However, they all suffer from great performance degradation due to the loss of discriminatory information during the translation from real space to binary space. Rathgeb et al. use LCSS (Linear Seprable Subcode) to extract binary representation of face template and apply a fuzzy vault scheme to protect it [39]. They claim around 32 bits false accept security analysed in FERET dataset[37]. Jiang et

al. in [19] also transform the face template to binary code but using computational secure sketch, which is based on DMSP assumption [15], to implement face-based authentication scheme and achieve considerable performance. However the assumption is new and might require more analysis to strengthen its security. And the scheme lacks the security analysis of irreversibility and unlinkability. **IronMask** [24], which can be abstract as a fuzzy commitment scheme, directly builds protection scheme on hypersphere without translating to binary space and achieve slight performance loss than other protection techniques based on ECC. They demonstrate that their scheme satisfies irreversibility, renewability and unlinkability to known attacks in their parameter settings when protecting **ArcFace**. Under particular settings, they claim that it can provide at least 115-bit security against known attacks.

### 2.3 Attack on Fuzzy-based Scheme

For secure sketch and fuzzy extractor on binary space, there have been analysis and attacks against the secure properties such as irreversibility, reusability and unlinkability. [4, 42] find that the original template can be recovered when getting multiple sketches from same template if the underlying error-correcting codes are different or biased. [42] finds an attack that can break the unlinkability of secure sketch. However, their attacks and analysis are focusing on the secure sketch within binary space and are not suitable for targeting the hypersphere. Until now, no efficient attack has been developed against the reusability and unlinkability of the secure sketch on the hypersphere.

## 3 REVISIT HYPERSPHERE ECC AND SECURE SKETCH

### 3.1 Notations

We denote the set  $\{1, 2, \dots, \rho\}$  as  $[\rho]$ . Denote general space/set, typically biometric template space, as math calligraphic such as  $\mathcal{M}$ . For particular space, we denote  $\mathbb{R}^n$  as  $n$ -dimension real-value space and  $S^{n-1}$  as hypersphere in  $\mathbb{R}^n$ . The vector in  $\mathbb{R}^n$  is denoted by bold small letter such as  $\mathbf{v}$  while the matrix is denoted by bold large letter such as  $\mathbf{M}$ . We denote the set of orthogonal matrices in  $\mathbb{R}^n$  as  $O(n)$  without any ambiguity with respect to the notation for complexity. The angle distance between two vectors  $\mathbf{v}, \mathbf{w}$  is defined as  $\text{Angle}(\mathbf{v}, \mathbf{w}) = \arccos\left(\frac{\mathbf{v} \cdot \mathbf{w}}{|\mathbf{v}| |\mathbf{w}|}\right)$ .

In this paper, we concentrate on the metric space  $S^{n-1}$  with  $\text{Angle}$  distance, as it is the embedding space of face template space  $\mathcal{M}$  of **ArcFace**.

### 3.2 HyperSphere Error Correct Code

Here we recall the definition of the HyperSphere-ECC, preparing for constructing hypersphere secure sketch.

*Definition 3.1 (HyperSphere-ECC [25]).* A set of codewords  $C \subset S^{n-1}$  is called HyperSphere-ECC if it satisfies:

- (1) (Discriminative)  $\forall \mathbf{c}_1, \mathbf{c}_2 \in C, \text{Angle}(\mathbf{c}_1, \mathbf{c}_2) > \theta$ ;
- (2) (Efficiently Decodable) There exists an efficient algorithm **Decode**, such that  $\forall \mathbf{c} \in C, \forall \mathbf{a} \in S^{n-1}$ , if  $\text{Angle}(\mathbf{a}, \mathbf{c}) < \frac{\theta}{2}$ , **Decode**( $\mathbf{a}$ ) =  $\mathbf{c}$ .

---

**Algorithm 1:** Sample and Decode Algorithms for HyperSphere-ECC  $C_\alpha$  in Definition 3.2

---

**Function Sample**( $n, \alpha$ )  $\rightarrow \mathbf{c}$

**Data:** dimension  $n$ , error parameter  $\alpha$

**Result:**  $\mathbf{c} \in C_\alpha$

Random choose  $\alpha$  distinct positions  $j_1, \dots, j_\alpha$ ;

$\mathbf{c} \leftarrow (0, \dots, 0)_n$ ;

**for**  $i \in \{j_1, \dots, j_\alpha\}$  **do**

$c_i \xleftarrow{\$} \{-\frac{1}{\sqrt{\alpha}}, \frac{1}{\sqrt{\alpha}}\}$ ;

Output  $\mathbf{c}$ ;

**Function Decode**( $\mathbf{u}, \alpha$ )  $\rightarrow \mathbf{c}$

**Data:**  $\mathbf{u} \in S^{n-1}$ , error parameter  $\alpha$

**Result:**  $\mathbf{c} \in C_\alpha$

Find the best  $\alpha$  positions  $J = \{j_1, \dots, j_\alpha\}$  such that

$\forall j \in J, \forall k \in [n] \setminus J |u_j| \geq |u_k|$ ;

$\mathbf{c} \leftarrow (0, \dots, 0)_n$ ;

**for**  $i \in J = \{j_1, \dots, j_\alpha\}$  **do**

$c_i \leftarrow \frac{u_i}{|u_i| \sqrt{\alpha}}$ ;

Output  $\mathbf{c}$ ;

---

In [25], Kim et al. devised a family of HyperSphere-ECC that can be efficiently sampled and decoded.

*Definition 3.2.* [25] For any positive integer  $\alpha$ ,  $C_\alpha$  is a set of codewords which have exactly  $\alpha$  non-zero entries. Each non-zero entries are either  $-\frac{1}{\sqrt{\alpha}}$  or  $\frac{1}{\sqrt{\alpha}}$ .

**THEOREM 3.3.** [25] *The designed distance  $\theta$  for  $C_\alpha$  is  $\frac{1}{2} \arccos(1 - \frac{1}{\alpha})$ .*

In real world, even for  $\mathbf{c} \in C$ ,  $\mathbf{a} \in S^{n-1}$ ,  $\text{Angle}(\mathbf{a}, \mathbf{c}) > \frac{\theta}{2}$ , there are chances that  $\text{Decode}(\mathbf{a}) = \mathbf{c}$ .

### 3.3 HyperSphere Secure Sketch and IronMask Scheme

Secure sketch was first proposed in [12]. It is a primitive that can precisely recover  $\mathbf{w}$  from any  $\mathbf{w}'$  close to  $\mathbf{w}$  with public information while not revealing too much information of  $\mathbf{w}$ . It has been a basic component to construct fuzzy extractor [12] and fuzzy commitment [21]. Here we recall the definition of the secure sketch.

*Definition 3.4 (Secure Sketch).* An  $(\mathcal{M}, t)$  secure sketch consists of a pair of algorithms (SS, Rec).

- The sketching algorithm SS takes input  $\mathbf{w} \in \mathcal{M}$ , outputs sketch  $s$  as public information.
- The recovery algorithm Rec takes input  $\mathbf{w}' \in \mathcal{M}$  and sketch  $s$ , outputs  $\mathbf{w}''$ .

It satisfies the following properties:

- Correctness: if  $\text{dis}(\mathbf{w}, \mathbf{w}') < t$ , then  $\text{Rec}(\mathbf{w}', \text{SS}(\mathbf{w})) = \mathbf{w}$ ;
- Security: It requires that sketch  $s$  does not leak too much information of  $\mathbf{w}$ , i.e.  $\max_{\mathbf{w}} \Pr[\mathbf{w}' | s = \text{SS}(\mathbf{w})] < \frac{1}{2^\lambda}$  in the sense of information view security. Or it's computational hard to retrieve  $\mathbf{w}$  given sketch  $s$ , i.e. for any Probabilistic

Polynomial Time(PPT) Adversary  $\mathcal{A}$ ,  $\Pr[\mathcal{A}(s = \text{SS}(\mathbf{w})) = \mathbf{w}] < \frac{1}{2^\lambda}$  in the sense of computational view security. ( $\lambda$  is security parameter)

For space  $\mathcal{F}^n$  with hamming distance, Dodis et al. proposes a general construction of secure sketch based on error-correcting code [12]. They also devise a general construction on the transitive space  $\mathcal{M}$ , i.e. for any  $a, b \in \mathcal{M}$ , there exists an isometry transformation  $\pi$  satisfying  $b = \pi(a)$ . Since hypersphere space is also transitive with orthogonal matrices, we can build a hypersphere secure sketch based on HyperSphere-ECC similar to error-correcting code.

*Definition 3.5 (HyperSphere Secure Sketch).* Given a HyperSphere-ECC  $C$  with decode algorithm **Decode** and design angle  $\theta$ , the hypersphere secure sketch can be constructed as below:

- Sketching algorithm **SS**: on input  $\mathbf{w} \in S^{n-1}$ ,  $\mathbf{c} \xleftarrow{\$} C$ , randomly generate an orthogonal matrix  $\mathbf{M}$  that satisfies  $\mathbf{c} = \mathbf{M}\mathbf{w}$ , output  $\mathbf{M}$  as sketch;
- Recovery algorithm **Rec**: on input  $\mathbf{w}' \in S^{n-1}$ , orthogonal matrix  $\mathbf{M}$ , compute  $\mathbf{v} \leftarrow \mathbf{M}\mathbf{w}'$ ,  $\mathbf{c}' \leftarrow \text{Decode}(\mathbf{v})$ , output  $\mathbf{w}'' \leftarrow \mathbf{M}^{-1}\mathbf{c}'$ .

It satisfies the following properties:

- Correctness: If  $\text{Angle}(\mathbf{w}, \mathbf{w}') < \frac{\theta}{2}$ ,  $\text{Angle}(\mathbf{M}\mathbf{w}, \mathbf{M}\mathbf{w}') < \frac{\theta}{2}$ . Based on the correctness of **Decode** algorithm, as  $\mathbf{M}\mathbf{w} = \mathbf{c}$ ,  $\mathbf{c}' = \text{Decode}(\mathbf{M}\mathbf{w}') = \mathbf{c}$ . Thus  $\mathbf{w}'' = \mathbf{M}^{-1}\mathbf{c}' = \mathbf{M}^{-1}\mathbf{c} = \mathbf{w}$ .
- Security: Since  $\mathbf{M}$  is randomized, if  $\mathbf{w}$  is uniformly distributed on  $S^{n-1}$ ,  $\{\mathbf{M}^{-1}\mathbf{c} | \forall \mathbf{c} \in C\}$  is set of all possible inputs with equal probability of SS. The probability for adversary guessing correct answer at one attempt is  $\frac{1}{|C|}$ .

In [25], they implement an algorithm named **hidden matrix rotation** to generate the random orthogonal matrix  $\mathbf{M}$  with constraint  $\mathbf{c} = \mathbf{M}\mathbf{w}$ .

*3.3.1 Tradeoff of Correctness and Security.* For secure sketch based on ECC, the error correcting capability of ECC is an important parameter to control the usability and the security of the whole algorithm. To achieve high security, the error correcting capability would be sacrificed so as usability. In [25], they choose  $\alpha = 16$  and  $n = 512$  to achieve  $|C| = \binom{n}{\alpha} \cdot 2^\alpha \approx 2^{115}$  security with average degrades 0.18% of true accept rate(TAR) at the same false accept rate(FAR) compared to facial recognition system without protection.

*3.3.2 Usage in Fuzzy Commitment and IronMask Scheme.* Secure sketch can be used in authentication combined with cryptographic hash function. The scheme is called fuzzy commitment[21]. The hash function is applied to secret codeword  $\mathbf{c}$  to get  $H(\mathbf{c})$  which is stored in the server. To authenticate to the server, the user only needs to recover the codeword as  $\mathbf{c}'$  by recovery algorithm of secure sketch, recompute  $H(\mathbf{c}')$  and send it back to the server. And server checks whether  $H(\mathbf{c}')$  and  $H(\mathbf{c})$  are equal. **IronMask**[24] utilizes this paradigm and replaces secure sketch by hypersphere secure sketch based on particular HyperSphere-ECC in Definition 3.2. Hash function is computationally secure if the probability of correctly guessing codeword  $\mathbf{c}$  in one trial is small. However, even for high probability of guessing secret codeword  $\mathbf{c}$  (e.g.  $2^{-40}$  if  $|C| = 2^{40}$ ), take advantage of slow hashes, such as PBKDF2 [32],

bcrypt [38] and scrypt [36], it's still inapplicable to implement exhausted searching attack, offering realistic security.

### 3.4 Threat Model

Here we define a game version of multiple usage security/reusability of secure sketch. Note that if  $t = 0$ , the multiple usage security degenerates to irreversibility.

*Definition 3.6.* Let  $SS = (SS, \text{Rec})$  be secure sketch's two algorithms. The experiment  $\text{SSMUL}_{\mathcal{A}, \theta, t}(n)$  is defined as follows:

- (1) The challenger  $C$  chooses a biometric resource  $\mathcal{W}$ , samples  $\mathbf{w} \in \mathcal{W}$  and sends  $SS(\mathbf{w})$  to adversary  $\mathcal{A}$ ;
- (2)  $\mathcal{A}$  asks  $q \leq t$  queries to challenger  $C$ .  $C$  samples  $\{\mathbf{w}_i \in \mathcal{W}, i = 1, \dots, q\}$  with constraints that  $\text{dis}(\mathbf{w}, \mathbf{w}_i) \leq \theta \wedge \text{dis}(\mathbf{w}_i, \mathbf{w}_j) \leq \theta, \forall i, j \in \{1, \dots, q\}$ , calculates the response set  $Q = \{SS(\mathbf{w}_i), i = 1, \dots, q\}$  and sends  $Q$  to  $\mathcal{A}$ ;
- (3)  $\mathcal{A}$  outputs  $\mathbf{w}'$ . If  $\mathbf{w}' = \mathbf{w}$ , outputs 1, else outputs 0.

The secure sketch is secure with  $(t+1)$  multiple usage if existing negligible function  $\text{negl}$  such that  $\Pr[\text{SSMUL}_{\mathcal{A}, \theta, t}(n) = 1] < \text{negl}(n)$  for all PPT adversaries  $\mathcal{A}$ .

The definition is very similar to the reusability of fuzzy extractor. However, our definition allows the attacker to control the distance of each sampled templates from same source while reusable fuzzy extractor does not [2, 45] or assumes too powerful attacker with ability to totally control shift distance between each templates in binary space [4]. We argue that our definition can more accurately capture the attacker's power to recover template in real scenarios. As in real world, the attacker is more probable to get multiple sketches from different servers but can not accurately control the shift distance enrolled each time. But it might get a vague quality report of each enrolled sketch and select the sketches that have similar qualities thus bounding the angle distance of pairs of corresponding unprotected templates, consistent with our security model.

## 4 PROBABILISTIC LINEAR REGRESSION ATTACK

### 4.1 Core Idea

Hypersphere secure sketch is secure from the information theoretical view in one-time usage. While if the same template  $\mathbf{w}$  is sketched multiple times, the sketches can determine the original  $\mathbf{w}$ .

For example, if  $\mathbf{w}$  is sketched twice, assume the sketches are  $\mathbf{M}_1, \mathbf{M}_2$  and corresponding codewords are  $\mathbf{c}_1, \mathbf{c}_2$ . The codeword pair  $(\mathbf{c}_1, \mathbf{c}_2)$  satisfies that  $\mathbf{c}_2 = \mathbf{M}_2 \mathbf{M}_1^{-1} \mathbf{c}_1$ . Since  $\mathbf{M}_1, \mathbf{M}_2$  are random orthogonal matrix,  $\mathbf{M} = \mathbf{M}_2 \mathbf{M}_1^{-1}$  can be seen as a random orthogonal matrix with only one constraint that maps  $\mathbf{c}_1$  to  $\mathbf{c}_2$ . Sparsity of the codewords implies there are few other pairs of  $(\mathbf{c}'_1, \mathbf{c}'_2)$  satisfying  $\mathbf{c}'_2 = \mathbf{M} \mathbf{c}'_1$ , so as corresponding template  $\mathbf{w}$ , otherwise  $\mathbf{M}$  should have other constraints and might even leak whole information of original template if  $\mathbf{M} \mathbf{c} \in C_\alpha \forall \mathbf{c} \in C_\alpha$  (see in Section 4.5). By exhaustive searching in the space of codewords, the pair  $(\mathbf{c}'_1, \mathbf{c}'_2)$  can be determined and the original template  $\mathbf{w}$  can be recovered as  $\mathbf{M}_1^{-1} \mathbf{c}'_1$ . Even if the structure of HyperSphere-ECC can be used, it's possible to downgrade the computation complexity of recovering  $\mathbf{w}$ .

Based on the HyperSphere-ECC construction employed by **Iron-Mask** in Definition 3.2, there have the designed distance  $\theta = \frac{1}{2} \arccos(1 - \frac{1}{\alpha})$ . For satisfactory accuracy, the codeword  $\mathbf{c}$  should utilize a small value of  $\alpha$  (specifically,  $n = 512, \alpha = 16$  are chosen). Therefore, the codewords contain a preponderance of  $(n - \alpha)$  zeros. From another view, given that matrix  $\mathbf{M}$  represents the output of the hypersphere secure sketch  $SS(\mathbf{w})$  and relates to the codeword  $\mathbf{c}$  via  $\mathbf{c} = \mathbf{M} \mathbf{w}$ , it follows that  $\mathbf{w}$  aligns orthogonally with a  $\frac{n-\alpha}{n}$  fraction of the row vectors in  $\mathbf{M}$ . It means that randomly selecting a row vector  $\mathbf{v}'$  from  $\mathbf{M}$  yields a  $\frac{n-\alpha}{n}$  probability that  $\mathbf{v}'$  is orthogonal to  $\mathbf{w}$ .

In the realm of linear algebra, determining the vector  $\mathbf{w} \in S^{n-1}$  necessitates a minimum of  $(n - 1)$  linear equations. Each sketch matrix  $\mathbf{M}$  derived from  $SS(\mathbf{w})$  offers a  $\frac{n-\alpha}{n}$  probability of correctly yielding a linear equation of the form  $\mathbf{w}^T \mathbf{v}' = 0$ . Therefore, if we possess  $(n - 1)$  sketches and randomly select a row vector from each, the probability of obtaining  $(n - 1)$  correct linear equations amounts to  $(\frac{n-\alpha}{n})^{n-1}$ , which approximates to  $e^{-\alpha}$  when  $\alpha \ll n$ . These equations are highly probably linear independent. Utilizing singular value decomposition(SVD), we can then deduce either the original vector  $\mathbf{w}$ (without noise) or a closely related vector  $\mathbf{w}'$ (with noise). Additionally, by utilizing the recovery algorithm of hypersphere secure sketch, we can reconstruct the original vector even when provided with a noisy solution  $\mathbf{w}'$ .

Furthermore, by fully exploiting HyperSphere-ECC inherent structure, we could reduce the number of required linear equations. Assuming that we possess  $n$  sketches relating to  $\mathbf{w}$ , denoted as  $\mathbf{M}_1, \mathbf{M}_2, \dots, \mathbf{M}_n$  with corresponding codewords  $\mathbf{c}_1, \mathbf{c}_2, \dots, \mathbf{c}_n$ . We can deduce the equations

$$\mathbf{c}_i = \mathbf{M}_i \mathbf{M}_1^{-1} \mathbf{c}_1, \forall 2 \leq i \leq n \quad (1)$$

Defining  $\mathbf{M}'_i = \mathbf{M}_i \mathbf{M}_1^{-1}$ , we can interpret  $\mathbf{M}'_i$  as sketches of  $\mathbf{c}_1$ . This allows us to solve for  $\mathbf{c}_1$  using  $(n - 1)$  linear equations. However, given that the entries of  $\mathbf{c}_1 \in C_\alpha$  predominantly consist of zeroes and that the non-zero entries possess uniform norms, the task of determining  $\mathbf{c}_1$  based on  $k$  linear equations can be seen as the **Subset Sum Problem** or the **Sparse Linear Regression Problem**. Numerous algorithms exist for tackling such problems, such as [10, 26, 40] for the **Subset Sum Problem** and [5, 6, 8, 13, 16, 17] for the **Sparse Linear Regression Problem**. We choose to use the Local Search Algorithm(LSA) introduced by Gamarnik and Zadik in [17] due to its effectiveness and simplicity of implementation. And other algorithms are more applicable when the coefficients of the linear equations are independent of the input vector( $\mathbf{c}_1$ ), which does not align with our specific problem where the equation's value is zero.

### 4.2 Details of Probabilistic Linear Regression Attack

The attack comprises three main components: the Linear Equation Sampler, the Linear Regression Solver, and the Threshold Determinant.

Initially, the linear equation sampler receives  $t$  sketches, denoted as  $\mathbf{M}_1, \mathbf{M}_2, \dots, \mathbf{M}_t$ , and sample rows from them to construct a single matrix  $\mathbf{M}$ . Subsequently, the linear regression solver processes this matrix  $\mathbf{M}$  and strives to generate a solution vector  $\mathbf{w}'$  satisfying

**Algorithm 2:** Linear Equation Sampler

---

**Data:** Matrices  $M_1, M_2, \dots, M_t \in \text{SS}(\cdot)$ , type = "SVD" or "LSA",  $k$

**Result:**  $M$

**if** type = "SVD" **then**

- $t' \leftarrow t$
- for**  $i = 1, \dots, t'$  **do**
  - $M'_i \leftarrow M_i$

**else if** type="LSA" **then**

- $t' \leftarrow t - 1$
- for**  $i = 1, \dots, t'$  **do**
  - $M'_i \leftarrow M_{i+1}M_1^{-1}$

$l \leftarrow \lfloor k/t' \rfloor$

**for**  $i = 1, \dots, t'$  **do**

- $\{v_{l(i-1)+j}^T | 1 \leq j \leq l\} \leftarrow$  Random select different  $l$  row vectors of  $M'_i$

**for**  $i = 1, \dots, k - l * t'$  **do**

- $\{v_{l * t' + i}^T\} \leftarrow$  Random select row vector different from already sampled vectors of  $M'_i$

$M \leftarrow$  vertical stack of  $v_1^T, v_2^T, \dots, v_k^T$

---

$\|Mw'\| \approx 0$ . Finally, the threshold determinant utilizes  $w'$  to recover candidate template  $w_r$  through recovery algorithm of secure sketch. This component then determines whether the recovered template is correct based on the predefined threshold  $\theta_t$  and the angle between  $w_r$  and  $w_{r'}$ , which is output of recovery algorithm with inputs of  $w_r$  and another sketch.

**4.2.1 Linear Equation Sampler.** The Linear Equation Sampler receives the sketches  $M_1, M_2, \dots, M_t$  derived from template  $w$  as input. Depending on the linear regression solver's chosen algorithm, the sampler selects row vectors from these sketches differently. If the solver employs the SVD algorithm, the sampler randomly picks  $k$  row vectors from the sketches. If solver uses LSA, the sampler first computes  $t - 1$  matrices  $M'_i = M_{i+1}M_1^{-1} \forall 2 \leq i \leq t$  and then randomly select  $k$  row vectors from these matrices. Subsequently, the sampler vertically stacks the chosen vectors to form the matrix  $M$  which is the input of the linear regression solver. The sampler's duty is to maximum the likelihood that  $\|Mw\| \approx 0$  (or  $\|MM_1w\| \approx 0$ ). We deem the matrix  $M$  as "correct" if for each selected row vector, the entry in corresponding mapped codeword is 0, where  $w$  represents original input template. "Correct" matrix ensures that  $\|Mw\| \approx 0$ .

*Definition 4.1.* In Algorithm 2, assume row vector  $v_i$  is sampled in  $m$ 'th row of matrix  $M'_j$  and the mapped codeword of  $M'_j$  is  $c$ , i.e.  $M'_j w = c$  if type = "SVD" where  $M_j = \text{SS}(w)$  or  $M_{j+1}w = c$  if type = "LSA" where  $M_{j+1} = \text{SS}(w)$ . We say the row vector  $v_i$  sampled by linear equation sampler is "correct" if and only if the  $m$ 'th entry of  $c$  is 0, i.e.  $c_m = 0$ . We say the sampled matrix  $M$  is "correct" if and only if all row vectors sampled are "correct". Otherwise,  $M$  is "incorrect".

**Algorithm 3:** Linear Regression Solver based on SVD

---

**Data:** Matrix  $M$  with size  $k * n$  where  $k \geq n - 1$

**Result:**  $w = \text{argmin}_w \|Mw\|$  where  $w \in S^{n-1}$

$w \leftarrow$  the eigenvector of matrix  $M$  with smallest eigenvalue

---

**Algorithm 4:** Linear Regression Solver based on Local Search Algorithm(LSA)

---

**Data:** Matrix  $M$  with size  $k * n$ , error correcting code parameter  $\alpha$ , hyper-parameter  $d, t_{th}$

**Result:**  $c$  or  $\perp$

$t \leftarrow 0$

**repeat**

- $c \leftarrow$  Random select codeword in  $C_\alpha$
- $t \leftarrow t + 1$
- repeat**
  - $norm_{pre} \leftarrow \|Mc\|$
  - $norm_{new} \leftarrow \|Mc\|$
  - for**  $c' \in C_\alpha$  where  $\|c' - c\| = \frac{\sqrt{2}}{\sqrt{\alpha}}$  **do**
    - $norm_{tmp} = \|Mc'\|$
    - if**  $norm_{tmp} < norm_{new}$  **then**
      - $norm_{new} \leftarrow norm_{tmp}, c_{new} \leftarrow c'$
  - $c \leftarrow c_{new}$
- until**  $norm_{new} = norm_{pre}$

**until**  $\|Mc\| \leq d$  or  $t > t_{th}$

**if**  $\|Mc\| \leq d$  **then**

- Output  $c$

**else**

- Output  $\perp$

---

**4.2.2 Linear Regression Solver.** The linear regression solver takes the output matrix  $M$  as input, solves the following optimization problem:

$$\text{argmin}_w \|Mw\|, w \in S^{n-1} \quad (2)$$

Two algorithms are employed : SVD(Singular Vector Decomposition) and LSA(Local Search Algorithm).

For SVD-based solver, a minimum of  $(n - 1)$  linear equations are required, and the output  $w'$  is a candidate solution for the original template. If only two sketches,  $M_1, M_2$ , are available in the step of linear equation sampler, an approximate solution of equation 2 can be obtained by solving a smaller matrix. When given 2 sketches, the task of linear equation sampler is equivalent to guessing  $\frac{k}{2}$  zero entries in each corresponding codewords  $c_1 = (c_1^1, c_2^1, \dots, c_n^1), c_2 = (c_1^2, c_2^2, \dots, c_n^2)$ , thus total  $k$  zero entries. Assuming  $U_1$  and  $U_2$  are the guessed set of zero-value entries in  $c_1$  and  $c_2$  respectively, and given that  $c_2 = M_2M_1^{-1}c_1$ , we can formulate a set of linear equations. These equations relate the non-zero entries of  $c_1$  to the zero entries of  $c_2$  through the matrix  $M_2M_1^{-1}$ . Therefore, assume  $M_2M_1^{-1} = (m_{ij})$ , we have

$$\sum_{j \notin U_1} m_{ij}c_j^1 = 0, \forall i \in U_2 \quad (3)$$

. By applying SVD, we could find a solution  $\mathbf{c}'$  that minimizes the squared error of these equations, subject to the constraint that the entries of  $\mathbf{c}'$  indexed by  $U_1$  are zero. The approximate solution for the original template is then given by  $\mathbf{w}' = \mathbf{M}_1^{-1}\mathbf{c}'$ . This approach reduces the matrix size from the original  $k * n$  to  $\frac{k}{2} * (n - \frac{k}{2})$  by at least factor 2 when  $k \geq n - 1$ .

For the LSA-based solver, the required number of linear equations exceeds  $\alpha \log n$  [17]. The solution obtained is a codeword  $\mathbf{c}' \in C_\alpha$ , and the candidate template solution is derived as  $\mathbf{M}_1^{-1}\mathbf{c}'$ .

**4.2.3 Threshold Determinant.** The threshold determinant obtains the solution template vector  $\mathbf{w}'$  from linear regression solver as an input and proceeds to attempt the recovery of the original template  $\mathbf{w}$ . Subsequently, it invokes the secure sketch's recovery algorithm utilizing  $\mathbf{w}'$  and the sketch  $\mathbf{M}_1$  to obtain candidate template  $\mathbf{w}_{r_1}$ . Then invoke the the secure sketch's recovery algorithm utilizing  $\mathbf{w}_{r_1}$  and the sketch  $\mathbf{M}_2$  to obtain another candidate template  $\mathbf{w}_{r_2}$ . Then the determinant calculates the angle  $\theta'$  as  $\text{Angle}(\mathbf{w}_{r_1}, \mathbf{w}_{r_2})$ . If  $\theta'$  surpasses a preset threshold  $\theta_t$ , the determinant returns a false output, indicating to the linear equation sampler that a new matrix should be generated for the linear regression solver to process. Otherwise, it outputs  $\mathbf{w}_{r_1}$  as the recovered solution template.

### 4.3 Correctness and Complexity Analysis

In this section, we present an analysis of the correctness and computational complexity of the probabilistic linear regression algorithm, specifically focusing on noiseless scenario. As for noisy environments, we demonstrate the practicality and efficiency of our algorithms through empirical experiments discussed in Section 5.

**4.3.1 Correctness.** The proof of the correctness of the probabilistic linear regression attack comprises three primary steps. First, we demonstrate that the inverse probability( $p_s$ ) of the output matrix  $\mathbf{M}$  from the linear equation sampler is "correct" in Definition 4.1, which satisfies  $\mathbf{M}\mathbf{w} = 0$ (or  $\mathbf{M}\mathbf{M}_1\mathbf{w} = 0$ ), is equal to  $2^{O(\alpha)}$ . Secondly, we establish that if the input matrix is "correct", the solution derived from linear regression solver is parallel to original template  $\mathbf{w}$ . Lastly, we show that the threshold determinant effectively filters out solutions  $\mathbf{w}'$  corresponding to "incorrect" sampled matrices.

Considering the linear equation sampler, let's assume the number of sampled rows is a multiple of the given matrices, i.e.  $k = l * t'$  ( $t' = t$  for SVD and  $t' = t + 1$  for LSA). The associated probability that  $l$  sampled row vectors from each matrix are orthogonal to template  $\mathbf{w}'$  is  $(\frac{l}{n})^l \geq (1 - \frac{\alpha}{n-l+1})^l$ . Consequently, the probability  $p_s$  of sampling all rows from  $t'$  matrices exceeds  $(1 - \frac{\alpha}{n-l+1})^{l * t'} = (1 - \frac{\alpha}{n-l+1})^k$ . Given practical conditions where  $\alpha \ll n$  and  $k \leq n - 1$ , we deduce that  $p_s \geq (1 - \frac{\alpha}{n-l+1})^k \geq (1 - \frac{\alpha}{n-l+1})^{n-1} \approx e^{-\frac{\alpha n}{n-l+1}}$ . Assume  $t'$  is greater than 2, we finally reach  $s_p \geq e^{-2\alpha}$ . Therefore, the inverse probability corresponds to  $2^{O(\alpha)}$ .

Considering the linear regression solver, assume the solution vector of input matrix  $\mathbf{M}$  is  $\mathbf{w}'$ . Leveraging the correctness of SVD algorithm, we have  $\mathbf{M}(\mathbf{w} - \mathbf{w}') = 0$  if  $\mathbf{M}$  is "correct". For the SVD-based solver, we require the dimension of matrix  $\mathbf{M}$  is  $(n - 1) * n$  to ensure a rank of  $(n - 1)$  with overwhelming probability. This guarantees that  $\mathbf{w}$  is parallel to  $\mathbf{w}'$ . For the LSA-based solver, if  $\mathbf{M}$

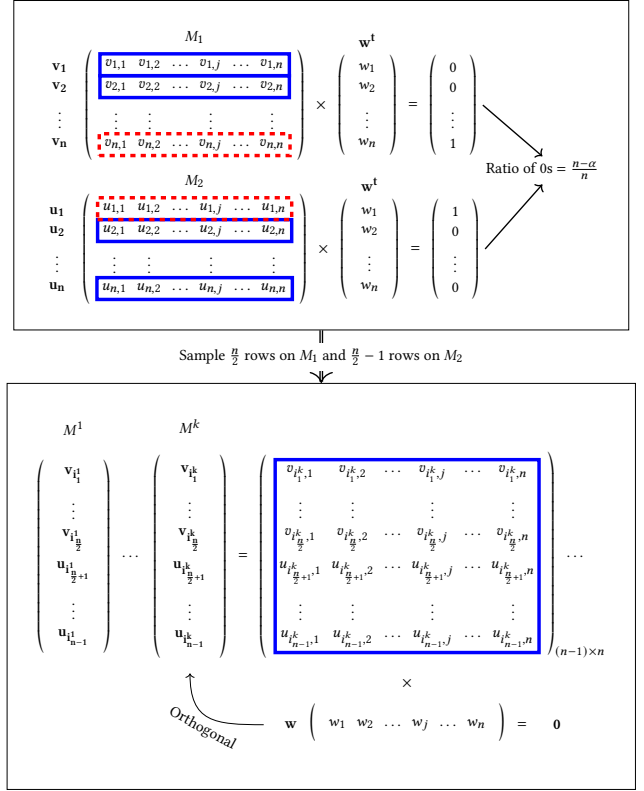


**Figure 1: Overview of probabilistic linear regression attack based on SVD on two matrices  $\mathbf{M}_1$  and  $\mathbf{M}_2$ .** The blue solid box indicates that the row vector is orthogonal to template  $\mathbf{w}$  while the red dashed box is not. By randomly selecting  $(n - 1)$  row vectors, we finally get matrix  $\mathbf{M}^k$  that  $\mathbf{w}$  is in null space of  $\mathbf{M}^k$ . As  $\mathbf{M}^k$  is full of rank, the only one null vector is parallel to  $\mathbf{w}$ .

is "correct", based on Theorem 2.7 from [17], for a sufficiently large  $k \geq \alpha \log(n)$  and small  $\sigma$  as  $n$  approaches infinity, we have the solution codeword  $\mathbf{c}'$  and original codeword  $\mathbf{c}$  satisfying  $\|\mathbf{c} - \mathbf{c}'\| \leq \sigma$  and  $\mathbf{c} = \mathbf{c}'$  for small enough  $\sigma$ . This implies that  $\mathbf{w}' = \mathbf{M}_1^{-1}\mathbf{c}'$  is parallel to  $\mathbf{M}_1^{-1}\mathbf{c} = \mathbf{w}$  (noting that  $-\mathbf{M}_1\mathbf{w}$  is also a valid solution for  $\arg\min_{\mathbf{x}} \|\mathbf{M}\mathbf{x}\|$ ).

Lastly, considering the threshold determinant, if the matrix sampled from linear equation sampler is "correct", assume the solution vector of SVD-based solver is  $\mathbf{w}'$  (for LSA-based solver, solution vector is  $\mathbf{w}' = \mathbf{M}_1^{-1}\mathbf{c}'$ ). We observe that  $\text{DECODE}(\mathbf{M}_i\mathbf{w}') = \text{DECODE}(\mathbf{w}'^T \cdot \mathbf{w}\mathbf{M}_i\mathbf{w}) = \mathbf{w}'^T \cdot \mathbf{w}\mathbf{M}_i\mathbf{w}$  and  $\mathbf{M}_i^{-1}\text{DECODE}(\mathbf{M}_i\mathbf{w}') = \mathbf{M}_i^{-1}\mathbf{w}'^T \cdot \mathbf{w}\mathbf{M}_i\mathbf{w} = \mathbf{w}'$ . Thus, we have

$$\mathbf{w}_{r_1} = \mathbf{M}_1^{-1}\text{DECODE}(\mathbf{M}_1\mathbf{w}') = \mathbf{w}' \quad (4)$$

$$\mathbf{w}_{r_2} = \mathbf{M}_2^{-1}\text{DECODE}(\mathbf{M}_2\mathbf{w}_{r_1}) = \mathbf{M}_2^{-1}\text{DECODE}(\mathbf{M}_2\mathbf{w}') = \mathbf{w}' \quad (5)$$

, ensuring a zero angle between  $\mathbf{w}_{r_1}$  and  $\mathbf{w}_{r_2}$ . Conversely, if the sampled matrix  $\mathbf{M}$  from linear equation sampler is "incorrect", the solution  $\mathbf{w}'$  of linear regression solver should deviate significantly

from the original template, making the candidate template  $w_{r_1}$  deviated from original template(both  $w$  and  $-w$ ). Thus  $w_{r_2} = \text{Rec}(w_{r_1})$  should also be deviated from  $w_{r_1}$ , otherwise we find another codeword pair  $c'_1 = M_1 w_{r_1}$  and  $c'_2 = M_2 w_{r_2}$  satisfying  $c'_1 = M_2 M_1^{-1} c'_2$ , which is impossible under the scenario that there are no other constraints for  $M_2$  and  $M_1$  but  $c_2 = M_2 M_1^{-1} c_1$  where  $M_2^{-1} c_2 = M_1^{-1} c_1 = w$ . Therefore, we could facilitate its exclusion through appropriate angle threshold settings.

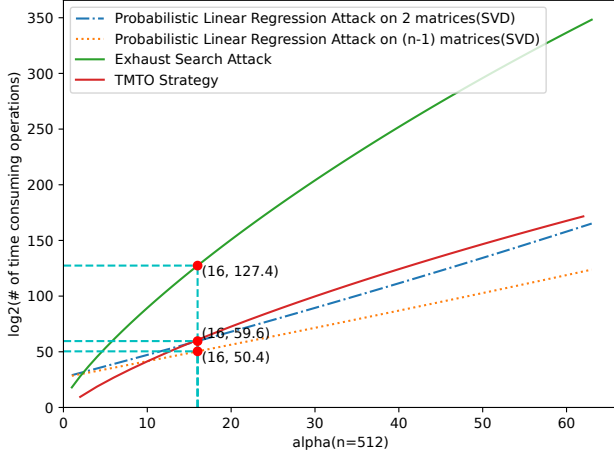


**Figure 2:**  $\log_2$  of the number of most time-consuming operations(complexity) of each algorithm according to different  $\alpha$  with  $n = 512$ . The complexity is  $O(n^3 e^\alpha)$  for Algorithm 3 and  $O(n^3 e^{2\alpha})$  for optimized SVD-based solver given 2 sketch in Section 4.2.2. Here we take the constant number in the complexity of SVD algorithm as 1. However, for concrete algorithms, the constant number might be 8 or more. As this number is constant and small, we argue that it does not influence our conclusions.

**4.3.2 Complexity.** In the context of the linear equation sampler, the inverse of the probability that the output matrix  $M$  is "correct", which satisfies the condition  $Mw = 0$ (or  $MM_1 w = 0$ ), is given by  $2^{O(\alpha)}$ , particularly  $e^\alpha$  when  $l$  equals to 1 and  $e^{2\alpha}$  when  $l$  equals to  $\frac{n}{2}$  where  $k = n - 1$  and  $l = k/t'$ . For the linear regression solver and threshold determinant components, the algorithms employed exhibit polynomial time complexity with respect to the matrix size  $n$ . Consequently, the overall time complexity of the entire algorithm can be expressed as  $2^{O(\alpha)} n^b$ , where  $b$  is a constant representing the degree of the polynomial time complexity.

When it comes to the SVD linear regression solver, the SVD algorithm exhibits time complexity of  $O(n^3)$  and it operates on a sampled matrix of dimension  $(n - 1) \times n$ . Considering the entire algorithm, the time complexity is  $O(e^\alpha n^3)$  for handling  $n - 1$  sketches, and  $O(e^{2\alpha} n^3)$  for handling 2 sketches.

Regarding the local search linear regression solver, each iteration carries a time complexity of  $O(n^2)$ . The maximum iteration count is influenced by factors such as  $\alpha$ ,  $\sigma$  and  $n$ , at least  $\alpha$  for random initial vector. Nevertheless, there is no explicit formula indicating

the precise number of equations necessary to arrive at accurate solutions. Consequently, determining the overall algorithm's complexity based on the local search method remains elusive. However, through empirical observations in Section 5, we hypothesize that the complexity of the local search-based algorithm is comparable to that of the SVD-based algorithm.

#### 4.4 Comparison with TMT0 Strategy

In [25], Kim et al. devise a time-memory-trade-off(TMT0) strategy to attack with two matrices, as solving  $c_2 = Mc_1$  for  $M = M_2 M_1^{-1}$ . The core idea is that each codeword  $c \in C_\alpha$  can be seen as a combination of two codewords  $c'_1$  and  $c'_2$  from  $C_{\frac{\alpha}{2}}$  with scalar  $\frac{1}{\sqrt{2}}$  as  $c_2 = \frac{1}{\sqrt{2}} (Mc'_1 + Mc'_2)$ . We only need to compute the smaller set  $\{Mc' | c' \in C_{\frac{\alpha}{2}}\}$  than exhaustive searching and check the pairs of  $c'$  and  $c''$  satisfied that the sum of  $Mc'$  and  $Mc''$  in particular entries are around 0,  $\pm \frac{\sqrt{2}}{\sqrt{\alpha}}$ . By utilizing particular sort algorithms, the pairs that need to be checked can be greatly reduced so as the complexity.

The obstacle of TMT0 strategy is that it needs substantial storage. For particular settings  $n = 512$ ,  $\alpha = 16$ , the required storage for storing codewords of  $C_8$  is at level EB. Considering the precision of the float number and noise in each sketching, to efficiently decrease the number of pairs to compare, the entries need to sum and sort would be more, making the storage requirement unacceptable.

Due to the significant storage demands of the TMT0 strategy, we chose not to implement it, focusing instead on providing a complexity analysis. As depicted in Figure 2, when compared to the TMT0 approach, our attack based on the SVD algorithm requires comparable computational resources when  $\alpha \geq 16$ ( $n = 512$ ) given two sketches, and less computational resources when  $\alpha < 16$ ( $n = 512$ ) given  $n - 1$  sketches if  $\alpha < 64$ . In specific scenarios ( $n = 512$ ,  $\alpha = 16$ ), the computational requirements under no noise of our algorithm are comparable to those of the TMT0 strategy, with our algorithm requiring approximately  $c * 2^{60}$  multiplications versus  $2^{60.8}$  additions of TMT0( $c$  is a small constant relative to the SVD algorithm used). Moreover, our algorithm requires only a small amount of constant storage space, in contrast to the TMT0 strategy, which demands large amounts of storage that are unacceptable in the proposed settings of IronMask. And the experiments in Section 5 demonstrate the effectiveness of our attacks while TMT0 strategy might be not effective in same noise levels. Therefore, we contend that our algorithm is the first practical attack on IronMask in the real world.

#### 4.5 Limit the Space of Secure Sketch

In Definition 3.5, the orthogonal matrix  $M$  does not have other constraints so that there only few pairs  $(c_1, c_2)$  satisfies  $c_2 = M_2 M_1^{-1} c_1$ . We may want that  $\forall w, \forall M_1, M_2 \in \text{SS}(w), \forall c \in C, M_2 M_1^{-1} c \in C$  so that the utilization of multiple sketches does not result in any additional information leakage beyond that of a single sketch. Then our attacks will not work. It requires that  $T = M_2 M_1^{-1}$  is not only an orthogonal matrix, but also maps  $C \rightarrow C$ . Here we give the format of matrices that maps  $C_\alpha \rightarrow C_\alpha$ (Proof seen in Appendix B).

**THEOREM 4.2.** *The form of orthogonal matrices  $\mathcal{T} = \{T: C_\alpha \rightarrow C_\alpha\}$  in  $\mathbb{R}^n$  with constraints  $\alpha \neq 2$  and  $\alpha \neq n$  is:*

$$(\pm \mathbf{e}_{i_1} \quad \pm \mathbf{e}_{i_2} \quad \cdots \quad \pm \mathbf{e}_{i_n}) \quad (6)$$

where  $\mathbf{e}_{i_1}, \mathbf{e}_{i_2}, \dots, \mathbf{e}_{i_n}$  is a permutation of unit vectors  $\mathbf{e}_0, \mathbf{e}_1, \dots, \mathbf{e}_n$ .

The remaining problem is how to choose  $\mathbf{M}_1$  such that  $\mathbf{TM}_1$  does not reveal too much information of template  $\mathbf{w}$ . One strategy is to use naive isometry rotation[24] to define  $\mathbf{M}_1$  by fixing the mapped codeword. However, we find an attack that can retrieve the template with almost 60% accuracy only given  $\mathbf{TM}_1$ (see in Appendix B). The other strategy is to define  $\mathbf{M}_1$  with randomness of  $\mathbf{w}$  and hash function  $H$ , i.e.  $\mathbf{M}_1 = H(\mathbf{w})$ . But the problem is that if  $H$  is sensitive to the difference of  $\mathbf{w}$ , it's still vulnerable to our probabilistic linear regression attack in noisy scenario(see in Section 5.2). Whether suitable orthogonal matrix given  $\mathbf{w}$  without leaking too much information exists remains an open problem.

## 5 EXPERIMENTS

We conduct experiments to attack **IronMask** protecting **ArcFace** with specifically parameter settings( $n = 512, \alpha = 16$ ). The experiments are carried out on a single laptop with Intel Core i7-12700H running at 2.30 GHz and 64 GB RAM. For SVD-based linear regression solver, we use the function `null_space` of python library `scipy`<sup>1</sup> and `svd` of `numpy`<sup>2</sup> library. For LSA-based linear regression solver, we implement using python and `numpy`<sup>3</sup> library.

Let  $r_k$  denote the expected number of matrices sampled by linear equation sampler until it samples the "correct" matrix  $\mathbf{M}$  in Definition 4.1. Let  $t_k$  denote the running time of linear regression solver that produces the solution of  $\arg\min_{\mathbf{w}} \|\mathbf{M}\mathbf{w}\|$  or terminates with a bot response. Define  $p_k$  as the probability that the solution obtained from linear regression solver passes the threshold determinant when the sampled matrix is "correct". Then the expected running time  $t_{all}$  of whole algorithm can be derived as  $t_{all} = r_k * t_k / p_k$ . As  $r_k$  could be calculated by formula  $r_k = \frac{1}{p_s}$  given  $n, k, \alpha$ , our task is to estimate  $t_k$  and  $p_k$  for varying number of equations  $k$  under specific scenario.

Note that LSA-based linear regression solver involves two iterations, and if the input matrix is "incorrect", the algorithm will reach the max number of outer iteration, denoted as  $t_{th}$ . Consequently, we have  $t_k = t_{th} * t_{in}$  where  $t_{in}$  is estimated running time of inner iteration. Assuming that the probability that LSA-based solver produces correct template in each outer iteration is  $p_{out}$ . The probability that LSA-based solver produces correct template given "correct" matrix before  $t_{th}$  iterations is  $1 - (1 - p_{out})^{t_{th}}$ . To minimize the overall running time is equal to minimizing  $\frac{t_{th}}{1 - (1 - p_{out})^{t_{th}}}$ . Hence, we arrive at  $t_{th} = \arg\min_t \frac{t}{1 - (1 - p_{out})^t}$ . Since  $0 < 1 - p < 1$ , we could deduce that  $t_{th} = 1$  and thus  $t_k = t_{in}$ .

### 5.1 Experiments in Noiseless Scenario

Since the expected iteration number  $r_k$  that linear equation sampler outputs "correct" matrix  $\mathbf{M}(\|\mathbf{M}\mathbf{w}\| \approx 0)$  and the running time of solver are both influenced by the number of sampled linear

equations( $k$ ), we conduct experiments to determine the optimal setting with the shortest expected time for various values of  $k$ .

We conduct experiments on the noiseless scenario in each sketching step, specifically with  $\theta = 0$  in Definition 3.6. The estimated running time are shown in Table 1. Our experiments indicate that for SVD-based probabilistic linear regression solver, the expected running time is approximately 1.7 year given only 2 sketches and 5.3 day given  $n - 1 = 511$  sketches. As for the LSA-based probabilistic linear regression solver, the minimum expected running time is 4.8 day with 3 sketches and 7.1 day with 281 sketches. The results demonstrate that our algorithms are practical to attack **IronMask** applied to protect **ArcFace** in noiseless scenario.

### 5.2 Experiments in Noisy Scenarios

In real-world, it's better suited that the templates sketched each time have noise between each other, i.e.  $\text{Angle}(\mathbf{M}_i^{-1}\mathbf{c}_i, \mathbf{M}_j^{-1}\mathbf{c}_j) < \theta'$  where  $\mathbf{c}_i, \mathbf{c}_j$  are corresponding codewords to  $\mathbf{M}_i, \mathbf{M}_j$ . For example, in FEI dataset[44], the angle distance between different poses(p03, p04, p05, p06, p07, p08, p11, p12) of same face is below  $36^\circ$  with 92% probability and below  $11^\circ$  with 0.3% probability.

We argue that our algorithms possess the capability to accommodate medium value  $\theta'$  with requirement of more iterations. Therefore, if the adversary have ability to choose sketches that maintain small angle distances within each corresponding original templates, they can still employ out attack to recover the original template.

However, upon consideration of noise, we discovered that even if the matrix is "correct", the threshold determinant alone cannot effectively discard solutions that deviate from the original template. This limitation arises because some candidate solutions  $\mathbf{w}_{r_1}$  which are close to original template exhibit the characteristic that  $\mathbf{M}_2\mathbf{w}_{r_1}$  are also close to the closest codeword, leading the algorithm to produce slight more candidate solutions. Nonetheless, there remains a high probability, denoted as  $p_f$ , that the output template of the algorithm is parallel to original template given a sampled "correct" matrix. Therefore, the expected running time  $t_{all}$  that the algorithm finally output template  $\mathbf{w}$  or  $-\mathbf{w}$  is revised as  $r_k * t_k / (p_k * p_f)$ . The corresponding results are shown in Table 3.

As  $k$  increases,  $r_k \times t_k$  grows exponentially, while  $\frac{1}{p_k \times p_f}$  decreases exponentially. Consequently, there exists a minimum  $t_{all}$  in the mid-range of  $k$ , like the noiseless scenario in Figure 3 with  $p_f = 1$ . Therefore, the Table 3 represents only the approximate minimum  $t_{all}$  in noisy environments.

Table 3 reveals that our algorithms require a greater number of sampled linear equations, resulting in increased expected running time. Nevertheless, it is important to note that these algorithms are fully parallelizable. Therefore, by deploying additional machines or leveraging high-performance computing resources, we can effectively parallelize the algorithms, enabling our algorithm to recover the template within an acceptable running time, even when faced with noise levels of  $36^\circ$ .

<sup>1</sup><https://scipy.org/>

<sup>2</sup><https://numpy.org/>

<sup>3</sup><https://numpy.org/>



**Table 1: The estimated expected running time for successfully retrieving template  $w$  or  $-w$  with an expected value of 1 are analysed across different parameters  $k$  with fixed  $n = 512$  for algorithms based on LSA-based solver in Algorithm 4 and SVD-based solver in Algorithm 3. Note that if the sketches are 2 for SVD-based solver, the algorithm is optimized mentioned in Section 4.2.2.  $t_k$  is approximated by computing the mean of the running time over 1000 iterations.  $p_k$  is estimated by calculating the proportion of successful times observed over maximum 20000 trials under the constraint that sampled matrix is "correct" in Definition 4.1.**

Algorithm	# sketches	$k$	$r_k$	Time( $t_k$ )	$p_k$	$\theta_t$	Time( $t_{all}$ )
SVD	2	511	$2^{32.6}$	8.4 ms	100%	$10^\circ$	1.7 year
	511		$2^{23.4}$	41ms	100%		5.3 day
LSA	3	220	$2^{11.35}$	102.0ms	$\frac{1}{1538.5}$	$10^\circ$	4.8 day
		240	$2^{12.54}$	108.6ms	$\frac{1}{833.3}$		6.2 day
		260	$2^{13.75}$	116.0ms	$\frac{1}{512.8}$		9.5 day
		280	$2^{15}$	130.0ms	$\frac{1}{219.8}$		10.9 day
	261	260	$2^{11.91}$	105ms	$\frac{1}{1666.7}$	$10^\circ$	7.8 day
	281	280	$2^{12.83}$	114ms	$\frac{1}{740.7}$		7.1 day
	301	300	$2^{13.74}$	123ms	$\frac{1}{454.5}$		8.86 day
	321	320	$2^{14.65}$	105ms	$\frac{1}{344.8}$		10.8 day

**Table 2: Estimated expected running time using LSA-based probabilistic linear regression attacker on Real-World Dataset.  $p_k * p_f$  is estimated by calculating the proportion of successful times observed over maximum 20000 trials under the constraint that sampled matrix is "correct" in Definition 4.1.**

Dataset	Noise( $\theta'$ )	$k$	$r_k$	Time( $t_k$ )	$p_k * p_f$	$\theta_t$	Time( $t_{all}$ )
FEI(p04, p05, p06)	$22.56^\circ$	300	$2^{16.29}$	131.8ms	$\frac{1}{847}$	$40^\circ$	103.7 day
FEI(p03, p05, p08)	$28.56^\circ$	340	$2^{18.97}$	129.0ms	$\frac{1}{697}$	$40^\circ$	1.47 year

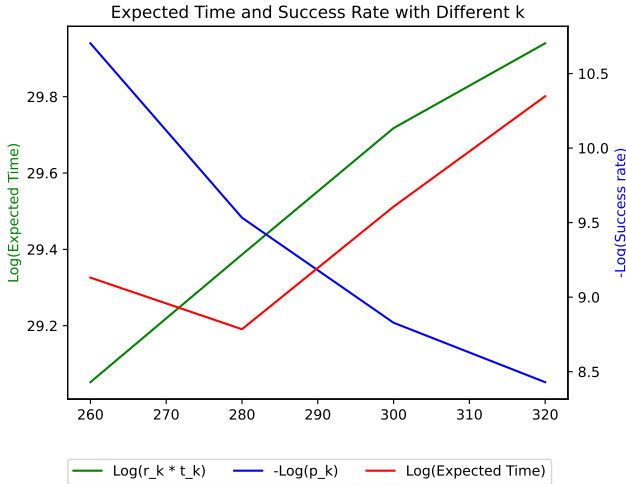


**Figure 3:  $\log_2(r_k * t_k)$ ,  $\log_2(\frac{1}{p_s})$ ,  $\log_2(t_{all})$  of different  $k$  using LSA-based attack algorithm when getting  $k + 1$  sketches in noiseless environments. The local minimum of  $t_{all}$  is reached as  $k \approx 280$ .**

### 5.3 Experiments in Real-World Dataset

Based on the previous section's findings, we have determined that the LSA-based linear regression solver exhibits superior performance. Therefore, we choose to employ the LSA-based attack algorithm, which necessitates the use of 3 sketches, for real-world simulations.

For our experiments, we select the FEI dataset, which utilizes the ArcFace neural network for feature extraction. The FEI face database is a Brazilian face database that contains 14 images for each of 200 individuals, thus a total of 2800 images. We choose 2 sets of poses (p03, p05, p08 and p04, p05, p06) to simulate noisy environment and constrained environment.

Table 2 shows that LSA-based probabilistic attack is applicable both in noisy environment and constrained environment, demonstrating the effectiveness of our attacks in real world.

## 6 DISCUSSION OF PLAUSIBLE DEFENSES

In the following content of this section, we discuss two strategies aimed at mitigating the impact of potential attacks against reusability. It is worth noting that these strategies are mutually independent, allowing us to combine them together to strengthen the hypersphere secure sketch against our attacks.

### 6.1 Add Extra Noise in Sketching Step

Our attacks and the TMTO strategy are effective primarily because the noise introduced between each sketching step is small, enabling

**Table 3: Estimated expected running time for different parameters  $\theta_t, k, p_k * p_f$  is estimated by calculating the proportion of successful times observed over maximum 20000 trials under the constraint that sampled matrix is "correct" in Definition 4.1.**

Noise( $\theta'$ )	Algorithm	# sketches	$k$	$r_k$	Time( $t_k$ )	$p_k * p_f$	$\theta_t$	Time( $t_{all}$ )
8.7°	SVD	2	522	$2^{34.6}$	7.0 ms	50%	40°	6 year
		531	531	$2^{24.32}$	33.9ms	78%		10.5 day
	LSA	3	240	$2^{12.54}$	110ms	$\frac{1}{800}$	30°	6.1 day
		321	320	$2^{14.65}$	112ms	$\frac{1}{350.9}$		11.8 day
14°	SVD	2	532	$2^{34.6}$	5.6 ms	25%	40°	18.9 year
		551	551	$2^{25.24}$	35.1ms	40%		40.2 day
	LSA	3	280	$2^{15.01}$	126ms	$\frac{1}{392}$	30°	18.8 day
		321	320	$2^{14.65}$	116ms	$\frac{1}{454.5}$		15.8 day
19°	SVD	2	552	$2^{36.57}$	5.3 ms	18%	40°	95 year
		591	591	$2^{27.06}$	36.6ms	26%		229.6 day
	LSA	3	280	$2^{15.01}$	129ms	$\frac{1}{833.4}$	30°	41 day
		321	320	$2^{14.65}$	115ms	$\frac{1}{1176.5}$		40.5 day
26°	SVD	2	592	$2^{40.8}$	4.4 ms	10%	40°	2676 year
		671	671	$2^{30.73}$	38.5ms	13.6%		16 year
	LSA	3	320	$2^{17.61}$	129ms	$\frac{1}{645.2}$	40°	193 day
		381	380	$2^{17.4}$	155ms	$\frac{1}{1111.1}$		346 day
30°	SVD	771	771	$2^{41.72}$	45.9 ms	42.2%	40°	147 year
		3	340	$2^{18.97}$	132ms	$\frac{1}{869.6}$	40°	1.87 year
	LSA	421	420	$2^{19.2}$	155ms	$\frac{1}{1428.6}$		4.34 year
		911	911	$2^{45.3}$	49.5 ms	13.4%	45°	$4.26 \times 10^4$ year
36°	SVD	3	380	$2^{21.82}$	145ms	$\frac{1}{2857.1}$	45°	48.65 year
		521	520	$2^{23.82}$	178ms	$\frac{1}{2222.2}$		185 year
	LSA	3	440	$2^{21.82}$	168ms	$\frac{1}{10000}$	50°	$4.8 \times 10^3$ year
		681	680	$2^{23.82}$	225ms	$\frac{1}{4851.75}$		$8.2 \times 10^4$ year

us to identify a limited number of codeword pairs  $(c_1, c_2)$  that meet the criterion of  $Angle(M_1^{-1}c_1, M_2^{-1}c_2)$  below a predefined threshold slightly larger than the estimated noise. However, if the noise between each sketching step becomes substantial enough to generate an excessive number of codeword pairs  $(c_1, c_2)$  satisfying the same angle threshold criterion, our attacks become ineffective. A straight method to increase the angle between two templates is to introduce additional random noise to them.

Assume three unit vectors are  $w_1, w_2$  and  $w_3$ , take  $\theta_{ij} = Angle(w_i, w_j)$ , then we have  $w_3 = \cos \theta_{13}w_1 + \sin \theta_{13}u$  and  $w_2 = \cos \theta_{12}w_1 + \sin \theta_{12}v$  where  $u$  and  $v$  are all unit vectors and  $w_1^T u = 0$  and  $w_1^T v = 0$ . We have

$$\begin{aligned} \cos \theta_{23} &= w_2^T w_3 = (\cos \theta_{13}w_1^T + \sin \theta_{13}u^T)(\cos \theta_{12}w_1 + \sin \theta_{12}v) \\ &= \cos \theta_{13} \cos \theta_{12} + \sin \theta_{13} \sin \theta_{12}u^T v \end{aligned}$$

If  $u$  or  $v$  is random, in expectation we have  $\cos \theta_{23} \approx \cos \theta_{13} \cos \theta_{12}$ .

Thus assume the initial noise between two templates  $w_1$  and  $w_2$  are  $\theta_i$ , the random noise added in sketching step is  $\theta_a$ , and the extra-noisy versions of two templates are  $w'_1$  and  $w'_2$ . We have  $\cos Angle(w'_1, w'_2) \approx \cos \theta_i \cos^2 \theta_a$  and  $\cos Angle(w'_1, w_2) \approx \cos \theta_i \cos \theta_a$ .

For user, template  $w_2$  is utilized to retrieve template  $w'_1$ . However, for an attacker, retrieve either  $w'_1$  or  $w'_2$  with corresponding sketches is necessary. The asymmetry in the noise encountered enables the user to still retrieve the template, while making it difficult

for the attacker to carry out attacks due to the presence of larger noise.

With a fixed template dimension of  $n = 512$ , we ensure that the distance between two templates, as perceived by an attacker, approximates the distance between a random unit vector and its nearest codeword, denoted as  $\theta_r$ . The relationship between the initial noise level and the success rate of the secure sketch recovery algorithm is in Table 4. The table shows that as  $\alpha$  decreases, while maintaining the same recovery success probability  $p_r$ , the initial noise  $\theta_i$  increases. Therefore, by fixing  $p_r$ , we can illustrate the relationship between  $\theta_i$  and  $\alpha$  in Figure 4.

Assume an initial noise level of  $36^\circ$ , which is the criterion for the FEI dataset, to maintain a recovery probability of approximately 90%, we find that  $\alpha \leq 6$ . This implies the brute-force space is reduced to less than  $2^{50.46}$ . However, if the attacker can obtain sketches from templates that are closer, the initial noise level should be lower than the criterion. For instance, in the FEI dataset, templates from poses p04, p05 and p06 are closer to each other than other poses. In such cases, the initial noise is  $22.56^\circ$ . To maintain the recovery probability high, we set  $\alpha = 5$ , achieving a recovery probability  $p_r = 95\%$  in the FEI dataset with poses(p03, p04, p05, p06, p07, p08, p11, p12). Here, the size of the brute-force attack space is reduced from  $2^{115}$  to  $2^{43}$ .

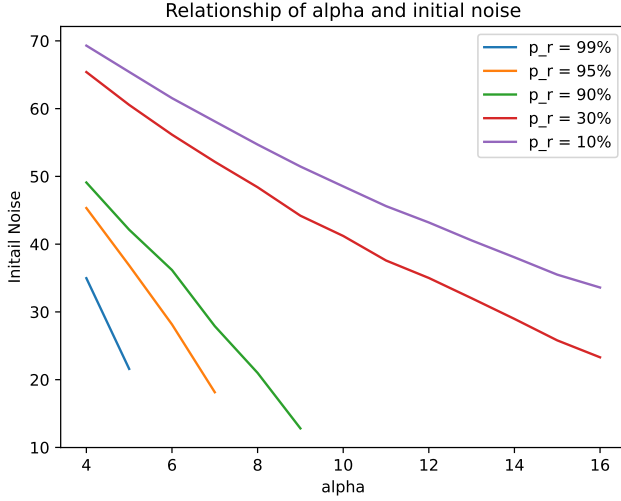


**Figure 4: The relationship of initial noise  $\theta_i$  and secure sketch parameter  $\alpha$  ( $n = 512$ ) with different recovery probability  $p_r$ .**

**Table 4: The relation between initial noise( $\theta_i$ ) and success rate( $p_r$ ) of recovery algorithm in secure sketch under different  $\alpha$  with  $n = 512$ . As  $\theta_r$  is expected noise in attackers' view which is equal to the distance between a random unit vector and its' nearest codeword, we have  $\cos \theta_r = \cos \theta_i \cos^2 \theta_a$ .**

$\alpha$	$\theta_i$	$\theta_a$	$p_r$	$\theta_r$	$\log_2( C_\alpha )$
16	$0^\circ$	$48.3^\circ$	56%	$63.8^\circ$	115
	$23.3^\circ$	$46.1^\circ$	30%		
	$33.6^\circ$	$43.2^\circ$	10%		
12	$0^\circ$	$50.9^\circ$	76%	$66.6^\circ$	91
	$34.8^\circ$	$45.9^\circ$	30%		
	$43.2^\circ$	$42.3^\circ$	10%		
8	$0^\circ$	$54.3^\circ$	95%	$70.1^\circ$	64
	$21.0^\circ$	$52.8^\circ$	90%		
	$48.4^\circ$	$44.2^\circ$	30%		
4	$54.7^\circ$	$39.8^\circ$	10%	$75.0^\circ$	35
	$0^\circ$	$59.4^\circ$	100%		
	$49.1^\circ$	$51.1^\circ$	90%		
	$65.4^\circ$	$38.2^\circ$	30%		
	$69.3^\circ$	$31.2^\circ$	10%		

## 6.2 Salting

To carry out attacks targeting reusability, a minimum of two protected templates is necessary. By incorporating randomness into our protection algorithm, we can effectively slow down the attack algorithm's progress. In the context of the hypersphere secure sketch algorithm, we propose appending  $n_{fake}$  additional random matrices, independent of the template  $\mathbf{w}$ , along with the output sketch matrix  $\mathbf{M}$ . Subsequently, the recovery process is modified to invoke recovery algorithm with these  $n_{fake} + 1$  matrices and take the recovery template closest to the input template as the final output.

From the attacker's perspective, acquiring two protected templates, each containing  $n_{fake} + 1$  matrices, necessitates the examination of  $(n_{fake} + 1)^2$  matrix pairs to employ the original attack algorithm. Consequently, we enhance the attack algorithm's complexity to a factor of  $\mathcal{O}(n_{fake}^2)$  at the cost of  $\mathcal{O}(n_{fake})$  times additional computations in recovery algorithm. In computational view, this enhancement is equal to augmenting security by  $\log_2(n_{fake})$  security bits.

For FEI dataset, if we take  $\alpha = 5$  in Section 6.1, the average runtime for recovery algorithm is  $2.16\mu\text{s}$ . To maintain the recovery time acceptable, we could take  $n_{fake} = 2^{20}$ . Then the time for recovery is approximate  $2\text{s}$  while the time for brute-force attacker to primarily attack secure sketch is  $2\text{s} * 2^{20} * 2^{43}/2 \approx 3.0 * 10^{12}$  year.

Due to the codeword space is shrinking to  $2^{43}$ , the fuzzy commitment scheme is not secure enough for directly solving  $\mathbf{c}$  from  $H(\mathbf{c})$  where  $\mathbf{c} \in C_\alpha$ . To enlarge the search space of hash function, we revise the commitment to be  $H(\mathbf{c}, \mathbf{M})$  to extend the search space from  $C_\alpha$  to  $C_\alpha \times \mathcal{S}_M$  where  $\mathbf{M}$  is the sketch of  $\mathbf{c}$  and  $\mathcal{S}_M$  contains  $\mathbf{M}$  and  $n_{fake}$  additional matrices. Thus for FEI dataset, the size of brute-force attacker's search space is  $2^{20+43} = 2^{63}$ . And if we set the time of hash function approximate  $2\text{s}$ , the complexity for directly attacking hash function is comparable to attacking secure sketch.

## 7 CONCLUSION

**IronMask** conceptualized as fuzzy commitment scheme is to protect the face template extracted by ArcFace in hypersphere, claims that it can provide at least 115-bit security against previous known attacks with great recognition performance. Targeting on renewability and unlinkability of **IronMask**, we proposed probabilistic linear regression attack that can successfully recover the original face template by exploiting the linearity of underlying used error correcting code. Under the recommended parameter settings on **IronMask** applied to protect **ArcFace**, our attacks are applicable in practical time verified by our experiments, even with the consistent noise level across biometric template extractions. To mitigate the impact of our attacks, we propose two plausible strategies for enhancing the hypersphere secure sketch scheme in **IronMask** at the cost of losses of security level and recovery success probabilities. To fully alleviate the error correcting code capability, future designs of hypersphere secure sketches and error-correcting codes should carefully consider the potential linearity of codewords, which may render them susceptible to attacks like the one we've presented.

## REFERENCES

- [1] Meng Ao and Stan Z. Li. 2009. Near Infrared Face Based Biometric Key Binding. In *Advances in Biometrics (Lecture Notes in Computer Science)*, Massimo Tistarelli and Mark S. Nixon (Eds.). Springer, Berlin, Heidelberg, 376–385. [https://doi.org/10.1007/978-3-642-01793-3\\_39](https://doi.org/10.1007/978-3-642-01793-3_39)
- [2] Daniel Apon, Chongwon Cho, Karim Eldefrawy, and Jonathan Katz. 2017. Efficient, Reusable Fuzzy Extractors from LWE. In *Cyber Security Cryptography and Machine Learning (Lecture Notes in Computer Science)*, Shlomi Dolev and Sachin Lodha (Eds.). Springer International Publishing, Cham, 1–18. [https://doi.org/10.1007/978-3-319-60080-2\\_1](https://doi.org/10.1007/978-3-319-60080-2_1)
- [3] Arathi Arakala, Jason Jeffers, and K. J. Horadam. 2007. Fuzzy Extractors for Minutiae-Based Fingerprint Authentication. In *Advances in Biometrics (Lecture Notes in Computer Science)*, Seong-Whan Lee and Stan Z. Li (Eds.). Springer, Berlin, Heidelberg, 760–769. [https://doi.org/10.1007/978-3-540-74549-5\\_80](https://doi.org/10.1007/978-3-540-74549-5_80)
- [4] Xavier Boyen. 2004. Reusable Cryptographic Fuzzy Extractors. In *Proceedings of the 11th ACM Conference on Computer and Communications Security*. ACM, Washington DC USA, 82–91. <https://doi.org/10.1145/1030083.1030096>

- [5] T. Tony Cai and Lie Wang. 2011. Orthogonal Matching Pursuit for Sparse Signal Recovery With Noise. *IEEE Transactions on Information Theory* 57, 7 (July 2011), 4680–4688. <https://doi.org/10.1109/TIT.2011.2146090>
- [6] Emmanuel J. Candès, Justin K. Romberg, and Terence Tao. 2006. Stable Signal Recovery from Incomplete and Inaccurate Measurements. *Communications on Pure and Applied Mathematics* 59, 8 (2006), 1207–1223. <https://doi.org/10.1002/cpa.20124>
- [7] R. Cappelli, D. Maio, A. Lumini, and D. Maltoni. 2007. Fingerprint Image Reconstruction from Standard Templates. *IEEE Transactions on Pattern Analysis and Machine Intelligence* 29, 9 (Sept. 2007), 1489–1503. <https://doi.org/10.1109/TPAMI.2007.1087>
- [8] Scott Shaobing Chen, David L. Donoho, and Michael A. Saunders. 1998. Atomic Decomposition by Basis Pursuit. *SIAM Journal on Scientific Computing* 20, 1 (1998), 33–61. <https://doi.org/10.1137/S1064827596304010> arXiv:<https://doi.org/10.1137/S1064827596304010>
- [9] S. Chopra, R. Hadsell, and Y. LeCun. 2005. Learning a Similarity Metric Discriminatively, with Application to Face Verification. In *2005 IEEE Computer Society Conference on Computer Vision and Pattern Recognition (CVPR'05)*, Vol. 1. IEEE, San Diego, CA, USA, 539–546. <https://doi.org/10.1109/CVPR.2005.202>
- [10] Matthijs J. Coster, Antoine Joux, Brian A. LaMacchia, Andrew M. Odlyzko, Claus-Peter Schnorr, and Jacques Stern. 1992. Improved Low-Density Subset Sum Algorithms. *computational complexity* 2, 2 (June 1992), 111–128. <https://doi.org/10.1007/BF01201999>
- [11] Jiankang Deng, Jia Guo, Jing Yang, Niannan Xue, Irene Kotsia, and Stefanos Zafeiriou. 2022. ArcFace: Additive Angular Margin Loss for Deep Face Recognition. *IEEE Transactions on Pattern Analysis and Machine Intelligence* 44, 10 (Oct. 2022), 5962–5979. <https://doi.org/10.1109/TPAMI.2021.3087709> arXiv:1801.07698 [cs]
- [12] Yevgeniy Dodis, Rafail Ostrovsky, Leonid Reyzin, and Adam Smith. 2008. Fuzzy Extractors: How to Generate Strong Keys from Biometrics and Other Noisy Data. *SIAM J. Comput.* 38, 1 (Jan. 2008), 97–139. <https://doi.org/10.1137/060651380> arXiv:cs/0602007
- [13] Simon Foucart and Holger Rauhut. 2013. *A Mathematical Introduction to Compressive Sensing*. Springer, New York, NY. <https://doi.org/10.1007/978-0-8176-4948-7>
- [14] Javier Galbally, Arun Ross, Marta Gomez-Barrero, Julian Fierrez, and Javier Ortega-Garcia. 2013. Iris Image Reconstruction from Binary Templates: An Efficient Probabilistic Approach Based on Genetic Algorithms. *Computer Vision and Image Understanding* 117, 10 (Oct. 2013), 1512–1525. <https://doi.org/10.1016/j.cviu.2013.06.003>
- [15] Steven D. Galbraith and Lukas Zobernig. 2019. Obfuscated Fuzzy Hamming Distance and Conjunctions from Subset Product Problems. In *Theory of Cryptography*, Dennis Hofheinz and Alon Rosen (Eds.), Vol. 11891. Springer International Publishing, Cham, 81–110. [https://doi.org/10.1007/978-3-030-36030-6\\_4](https://doi.org/10.1007/978-3-030-36030-6_4)
- [16] David Gamarnik, Eren C. Kizildag, and Ilias Zadik. 2021. Inference in High-Dimensional Linear Regression via Lattice Basis Reduction and Integer Relation Detection. *IEEE Transactions on Information Theory* 67, 12 (Dec. 2021), 8109–8139. <https://doi.org/10.1109/TIT.2021.3113921> arXiv:1910.10890 [math, stat]
- [17] David Gamarnik and Ilias Zadik. 2019. Sparse High-Dimensional Linear Regression. Algorithmic Barriers and a Local Search Algorithm. arXiv:1711.04952 [math, stat]
- [18] Abhishek Jana, Bipin Paudel, Md. Kamruzzaman Sarker, Monireh Ebrahimi, Pascal Hitzler, and George T. Amariuca. 2022. Neural Fuzzy Extractors: A Secure Way to Use Artificial Neural Networks for Biometric User Authentication. *Proc. Priv. Enhancing Technol.* 2022, 4 (2022), 86–104. <https://doi.org/10.56553/POPETS-2022-0100>
- [19] Mingming Jiang, Shengli Liu, You Lyu, and Yu Zhou. 2023. Face-Based Authentication Using Computational Secure Sketch. *IEEE Transactions on Mobile Computing* 22, 12 (2023), 7172–7187. <https://doi.org/10.1109/TMC.2022.3207830>
- [20] Ari Juels and Madhu Sudan. 2006. A Fuzzy Vault Scheme. *Designs, Codes and Cryptography* 38, 2 (Feb. 2006), 237–257. <https://doi.org/10.1007/s10623-005-6343-z>
- [21] Ari Juels and Martin Wattenberg. 1999. A Fuzzy Commitment Scheme. In *Proceedings of the 6th ACM Conference on Computer and Communications Security (CCS '99)*. Association for Computing Machinery, New York, NY, USA, 28–36. <https://doi.org/10.1145/319709.319714>
- [22] Shuichi Katsumata, Takahiro Matsuda, Wataru Nakamura, Kazuma Ohara, and Kenta Takahashi. 2021. Revisiting Fuzzy Signatures: Towards a More Risk-Free Cryptographic Authentication System Based on Biometrics. In *Proceedings of the 2021 ACM SIGSAC Conference on Computer and Communications Security (CCS '21)*. Association for Computing Machinery, New York, NY, USA, 2046–2065. <https://doi.org/10.1145/3460120.3484586>
- [23] Christof Kauba, Simon Kirchgasser, Vahid Mirjalili, Andreas Uhl, and Arun Ross. 2021. Inverse Biometrics: Generating Vascular Images From Binary Templates. *IEEE Transactions on Biometrics, Behavior, and Identity Science* 3, 4 (Oct. 2021), 464–478. <https://doi.org/10.1109/TBIOM.2021.3073666>
- [24] Sunpill Kim, Yunseong Jeong, Jinsu Kim, Jungkon Kim, Hyung Tae Lee, and Jae Hong Seo. 2021. IronMask: Modular Architecture for Protecting Deep Face Template. arXiv:2104.02239 [cs]
- [25] Sunpill Kim, Yunseong Jeong, Jinsu Kim, Jungkon Kim, Hyung Tae Lee, and Jae Hong Seo. 2021. IronMask: Modular Architecture for Protecting Deep Face Template. In *2021 IEEE/CVF Conference on Computer Vision and Pattern Recognition (CVPR)*. IEEE, Nashville, TN, USA, 16120–16129. <https://doi.org/10.1109/CVPR46437.2021.01586>
- [26] J. C. Lagarias and A. M. Odlyzko. 1985. Solving Low-Density Subset Sum Problems. *J. ACM* 32, 1 (Jan. 1985), 229–246. <https://doi.org/10.1145/2455.2461>
- [27] Youn Joo Lee, Kwanghyuk Bae, Sung Joo Lee, Kang Ryoung Park, and Jaihee Kim. 2007. Biometric Key Binding: Fuzzy Vault Based on Iris Images. In *Advances in Biometrics (Lecture Notes in Computer Science)*, Seong-Whan Lee and Stan Z. Li (Eds.). Springer, Berlin, Heidelberg, 800–808. [https://doi.org/10.1007/978-3-540-74549-5\\_84](https://doi.org/10.1007/978-3-540-74549-5_84)
- [28] Weiyang Liu, Yandong Wen, Zhiding Yu, Ming Li, Bhiksha Raj, and Le Song. 2017. SphereFace: Deep Hypersphere Embedding for Face Recognition. <https://arxiv.org/abs/1704.08063v4>.
- [29] Guangan Mai, Kai Cao, Pong C. Yuen, and Anil K. Jain. 2019. On the Reconstruction of Face Images from Deep Face Templates. *IEEE Transactions on Pattern Analysis and Machine Intelligence* 41, 5 (May 2019), 1188–1202. <https://doi.org/10.1109/TPAMI.2018.2827389> arXiv:1703.00832 [cs]
- [30] Qiang Meng, Shichao Zhao, Zhida Huang, and Feng Zhou. 2021. MagFace: A Universal Representation for Face Recognition and Quality Assessment. In *2021 IEEE/CVF Conference on Computer Vision and Pattern Recognition (CVPR)*. IEEE, Nashville, TN, USA, 14220–14229. <https://doi.org/10.1109/CVPR46437.2021.01400>
- [31] Deen Dayal Mohan, Nishant Sankaran, Sergey Tulyakov, Srirangaraj Setlur, and Venu Govindaraju. 2019. Significant Feature Based Representation for Template Protection. In *2019 IEEE/CVF Conference on Computer Vision and Pattern Recognition Workshops (CVPRW)*. IEEE, Long Beach, CA, USA, 2389–2396. <https://doi.org/10.1109/CVPRW.2019.00293>
- [32] Kathleen Moriarty, Burt Kaliski, and Aneas Rusch. 2017. *PKCS #5: Password-Based Cryptography Specification Version 2.1*. Request for Comments RFC 8018. Internet Engineering Task Force. <https://doi.org/10.17487/RFC8018>
- [33] Hatif Otroshi Shahreza, Vedrana Krivokuća Hahn, and Sébastien Marcel. 2024. Vulnerability of State-of-the-Art Face Recognition Models to Template Inversion Attack. *IEEE Transactions on Information Forensics and Security* 19 (2024), 4585–4600. <https://doi.org/10.1109/TIFS.2024.3381820>
- [34] Hatif Otroshi Shahreza and Sébastien Marcel. 2023. Face Reconstruction from Facial Templates by Learning Latent Space of a Generator Network. In *Advances in Neural Information Processing Systems*, A. Oh, T. Naumann, A. Globerson, K. Saenko, M. Hardt, and S. Levine (Eds.), Vol. 36. Curran Associates, Inc., New Orleans, LA, USA, 12703–12720. [https://proceedings.neurips.cc/paper\\_files/paper/2023/file/29e4b51d45dc8f534260adc45b587363-Paper-Conference.pdf](https://proceedings.neurips.cc/paper_files/paper/2023/file/29e4b51d45dc8f534260adc45b587363-Paper-Conference.pdf)
- [35] Rohit Kumar Pandey, Yingbo Zhou, Bhargava Urala Kota, and Venu Govindaraju. 2016. Deep Secure Encoding for Face Template Protection. In *2016 IEEE Conference on Computer Vision and Pattern Recognition Workshops (CVPRW)*. IEEE, Las Vegas, NV, USA, 77–83. <https://doi.org/10.1109/CVPRW.2016.17>
- [36] Colin Percival and Simon Josefsson. 2016. *The Scrypt Password-Based Key Derivation Function*. Request for Comments RFC 7914. Internet Engineering Task Force. <https://doi.org/10.17487/RFC7914>
- [37] P. Jonathan Phillips, Harry Wechsler, Jeffery Huang, and Patrick J. Rauss. 1998. The FERET Database and Evaluation Procedure for Face-Recognition Algorithms. *Image and Vision Computing* 16, 5 (April 1998), 295–306. [https://doi.org/10.1016/S0262-8856\(97\)00070-X](https://doi.org/10.1016/S0262-8856(97)00070-X)
- [38] Niels Provos and David Mazières. 1999. A Future-Adaptable Password Scheme. In *1999 USENIX Annual Technical Conference (USENIX ATC 99)*. USENIX Association, Monterey, CA, 81–91. <http://www.usenix.org/events/usenix99/provos.html>
- [39] Christian Rathgeb, Johannes Merkle, Johanna Scholz, Benjamin Tams, and Vanessa Nesterowicz. 2022. Deep Face Fuzzy Vault: Implementation and Performance. *Computers & Security* 113 (Feb. 2022), 102539. <https://doi.org/10.1016/j.cose.2021.102539>
- [40] C. P. Schnorr and M. Euchner. 1994. Lattice basis reduction: improved practical algorithms and solving subset sum problems. *Math. Program.* 66, 2 (sep 1994), 181–199. <https://doi.org/10.1007/BF01581144>
- [41] Florian Schroff, Dmitry Kalenichenko, and James Philbin. 2015. FaceNet: A unified embedding for face recognition and clustering. In *IEEE Conference on Computer Vision and Pattern Recognition, CVPR 2015, Boston, MA, USA, June 7-12, 2015*. IEEE Computer Society, Boston, MA, USA, 815–823. <https://doi.org/10.1109/CVPR.2015.7298682>
- [42] Koen Simoons, Pim Tuyls, and Bart Preneel. 2009. Privacy Weaknesses in Biometric Sketches. In *2009 30th IEEE Symposium on Security and Privacy*. IEEE, Oakland, CA, USA, 188–203. <https://doi.org/10.1109/SP.2009.24>
- [43] Veeru Talreja, Matthew C. Valenti, and Nasser M. Nasrabadi. 2019. Zero-Shot Deep Hashing and Neural Network Based Error Correction for Face Template Protection. In *2019 IEEE 10th International Conference on Biometrics Theory, Applications and Systems (BTAS)*. IEEE, Tampa, FL, USA, 1–10. <https://doi.org/10.1109/BTAS46853.2019.9185979>
- [44] Carlos Eduardo Thomaz and Gilson Antonio Giraldi. 2010. A New Ranking Method for Principal Components Analysis and Its Application to Face Image

Analysis. *Image and Vision Computing* 28, 6 (June 2010), 902–913. <https://doi.org/10.1016/j.imavis.2009.11.005>

[45] Yunhua Wen, Shengli Liu, and Shuai Han. 2018. Reusable Fuzzy Extractor from the Decisional Diffie–Hellman Assumption. *Designs, Codes and Cryptography* 86, 11 (Nov. 2018), 2495–2512. <https://doi.org/10.1007/s10623-018-0459-4>

## A TMTO STRATEGY

In [25], they describe a time-memory trade-off(TMTO) strategy to attack IronMask, here we revise the details of TMTO strategy to make it more applicable in real world's settings.

Assume  $\mathbf{M}_1$  and  $\mathbf{M}_2$  are two sketches of biometric template  $\mathbf{w}$ , our target is to find codeword pair  $(\mathbf{c}_1, \mathbf{c}_2)$  in  $C_\alpha$  such that  $\mathbf{c}_2 = \mathbf{M}\mathbf{c}_1$  for orthogonal matrix  $\mathbf{M} = \mathbf{M}_2\mathbf{M}_1^{-1}$ . Let  $\mathbf{c}_1 = (c_{11}, c_{12}, \dots, c_{1n})$ ,  $\mathbf{c}_2 = (c_{21}, c_{22}, \dots, c_{2n})$  and  $\mathbf{M} = (m_{ij})$ . The equation can be rewritten as

$$c_{11}m_{i1} + c_{12}m_{i2} + \dots + c_{1n}m_{in} = c_{2i}, \forall 1 \leq i \leq n \quad (7)$$

. As each codeword  $\mathbf{c} \in C_\alpha$  can be written as two components  $\mathbf{a}, \mathbf{b}$  where each has exactly  $\frac{\alpha}{2}$  non-zero elements and there is no positions that both  $\mathbf{a}$  and  $\mathbf{b}$  are non-zero. We can rewrite Equation(7) as

$$\sum_{\mathbf{a}=(a_1, \dots, a_n) \in C_{\frac{\alpha}{2}}} a_j m_{ij} + \sum_{\mathbf{b}=(b_1, \dots, b_n) \in C_{\frac{\alpha}{2}}} b_j m_{ij} = \sqrt{2}c_{2i}, \forall 1 \leq i \leq n \quad (8)$$

with constraint  $\sqrt{2}\mathbf{c}_1 = \mathbf{a} + \mathbf{b}$ . If we relax the constraint to that  $\mathbf{a}$  and  $\mathbf{b}$  have exactly  $\frac{\alpha}{2}$  non-zero elements, the Equation(8) can be simplified as

$$\sum_{\mathbf{a} \in C_{\frac{\alpha}{2}}} a_j m_{ij} = \sqrt{2}c_{2i} - \sum_{\mathbf{b} \in C_{\frac{\alpha}{2}}} b_j m_{ij}, \forall 1 \leq i \leq n \quad (9)$$

. As there are three elements  $-\frac{1}{\sqrt{\alpha}}, 0, \frac{1}{\sqrt{\alpha}}$  for  $c_{2i}$  and with high probability  $c_{2i} = 0$  if  $\alpha \ll n$ , we can just assume  $c_{2i} = 0$  for random selected  $i$ . Then we calculate all  $t_a^i = \sum_{\mathbf{a} \in C_{\frac{\alpha}{2}}} a_j m_{ij}$  for some  $i$ , search them and find pairs that satisfies  $t_a^i + t_b^i = 0$  for  $\mathbf{a}, \mathbf{b} \in C_{\frac{\alpha}{2}}$ . As  $t_a^i = -t_{-a}^i$ , it only needs to find  $\mathbf{a}, \mathbf{b} \in C_{\frac{\alpha}{2}}$  such that  $t_a^i = t_b^i$ . The possible codeword  $\mathbf{c}_1$  is equal to  $\frac{1}{\sqrt{2}}(\mathbf{a} - \mathbf{b})$ .

In real world, since  $t_a$  is float number with limited precision and there's some noise in  $c_{2i}$  in real settings, to make TMTO strategy work in these scenarios, we should calculate more  $t_a$  for different  $i$ 's and search by bucket with round-up.

The precise description of TMTO strategy attack is below:

- (1)  $\forall a \in C_{\frac{\alpha}{2}}$ , calculate the  $t_a^i = \sum a_j m_{ij}$  for chosen  $i$ 's;
- (2) search  $t_a^i$  by bucket search or other search algorithms;
- (3) find all different codewords  $(\mathbf{a}, \mathbf{b})$  that satisfies  $t_a^i = t_b^i$  for all chosen  $i$ 's, check whether  $t_a^i = t_b^i + x, \forall 1 \leq i \leq n$  where  $x = -\frac{\sqrt{2}}{\sqrt{\alpha}}, 0, \frac{\sqrt{2}}{\sqrt{\alpha}}$  and output  $\frac{1}{\sqrt{2}}(\mathbf{a} - \mathbf{b})$  as codeword  $\mathbf{c}_1$ .

**Complexity** The probability that the equation  $t_a^i = t_b^i$  is correct for random  $i$  is  $\frac{n-\alpha}{n}$ . The number of codewords  $C_{\frac{\alpha}{2}}$  is  $2^{\frac{\alpha}{2}} \binom{n}{\frac{\alpha}{2}}$ . For each codeword in  $C_{\frac{\alpha}{2}}$ , it needs  $\frac{\alpha}{2}$  additions to compute  $t^i$ . Thus, with success expectation of 1, we need total  $\frac{\alpha n}{2(n-\alpha)} |C_{\frac{\alpha}{2}}|$  additions and also need memory to store  $|C_{\frac{\alpha}{2}}|$  codewords with  $t^i$ . If the step 1-3 can be done together, we can early terminate the calculation of step 2 if satisfactory pairs of codewords have found. As for codeword

$\mathbf{c}_1 \in C_\alpha$ , there are  $\binom{\alpha}{\frac{\alpha}{2}}$  pairs in  $C_{\frac{\alpha}{2}}$  that sums to  $\sqrt{2}\mathbf{c}_1$ . Therefore, the storage requirement and number of additions can be decreased by factor  $\sqrt{\binom{\alpha}{\frac{\alpha}{2}}}$ .

Here we assume that there are few pairs satisfying the conditions in step 3. However, since the precision of  $t^i$  is limited, the satisfying pairs might be too large, making the computation cost of checking each pairs on other entries unacceptable. For example, if  $t^i$  is 32-bit format float and distributed in range  $(-1, 1)$ , it can only exclude magnitude of  $2^{33}$  pairs of codewords. Thus, to exclude enough pairs of codewords, we need to calculate  $t^i$  for more different  $i$ 's. It will slightly enlarge the storage requirement with factor  $\#i$ (number of chosen  $i$ 's) and number of additions with factor  $\#i * \left(\frac{n}{n-\alpha}\right)^{\#i}$ . If the the equation 7 contains some noise, the required number of  $i$ 's would be more.

We ignore the complexity of search algorithm. As if the search algorithm is bucket search, the time and storage complexity is  $O(|C_{\frac{\alpha}{2}}|)$ , comparable to the complexity of additions.

For concrete settings as  $n = 512, \alpha = 16$ , the requirement of storage is around  $2^{57.8}$  codewords and each codeword needs  $8 * \log_2(512) = 72$  bit = 9 bytes with at least 4 bytes for storage of  $t^i$ , which makes the storage larger than 2.8 EB. And the requirement of additions is around  $2^{60.8}$ .

## B REMARK ON LIMITED SPACE OF SECURE SKETCH

Here we give an attack if the sketch is generated as in Section 4.5, i.e.  $\text{SS}(\mathbf{w}) = \text{TM}_1$  where  $\mathbf{M}_1$  is naive rotation matrix from  $\mathbf{w}$  to predefined fixed codeword  $\mathbf{c}_{fixed}$  and  $\mathbf{T}$  is defined in Theorem 4.2. First, we give the proof of the Theorem 4.2.

**THEOREM 4.2.** Assume  $\mathbf{T} = (t_{ij}), \mathbf{a} = (a_1, \dots, a_n) \in C_\alpha$  where  $a_j = \frac{1}{\sqrt{\alpha}}$ . Then  $\mathbf{a}' = (a'_1, \dots, a'_n) \in C_\alpha$  where  $\forall k \neq j, a'_k = a_k$  and  $a'_j = -a_j$ . Because of the definition of  $\mathbf{T}, \mathbf{T}\mathbf{a}, \mathbf{T}\mathbf{a}' \in C_\alpha$ . We have

$$\mathbf{T}\mathbf{a} - \mathbf{T}\mathbf{a}' = \mathbf{c} - \mathbf{c}' \quad (10)$$

$$\frac{2}{\sqrt{\alpha}} t_{ij} = \pm \frac{2}{\sqrt{\alpha}}, \pm \frac{1}{\sqrt{\alpha}}, 0 \quad (11)$$

$$t_{ij} = \pm 1, \pm 0.5, 0 \quad (12)$$

$\forall i, j \in [n]$ . Since  $\mathbf{T}$  is an orthogonal matrix, the norm of each row of  $\mathbf{T}$  is 1. There are two cases for each row of  $\mathbf{T}$ . One is that it consists of four positions filled with  $\pm 0.5$ , the other is that it only has one position filled with  $\pm 1$ . Here we prove that the first case is unsatisfactory by showing that if exist row  $i$  of  $\mathbf{T}$  satisfies first case,  $\exists \mathbf{c} \in C_\alpha, \mathbf{T}\mathbf{c} \notin C_\alpha$ .

For row  $i$  of  $\mathbf{T}$ , assume  $t_{ij_1}, t_{ij_2}, t_{ij_3}, t_{ij_4} = \pm 0.5$ . If  $\alpha = 1, t_{i*} * \mathbf{c} = 0.5$  with  $c_{j_1} = 1$ . Then  $\mathbf{T}\mathbf{c} \notin C_\alpha$ . If  $\alpha \geq 3$ , construct  $\mathbf{c} \in C_\alpha$  so that  $\forall 1 \leq k \leq 3, c_{j_k} = \text{sign}(t_{ij_k}) \frac{1}{\sqrt{\alpha}}$  and  $c_{j_4} = 0$ . Then  $t_{i*} * \mathbf{c} = \frac{3}{2\sqrt{\alpha}}$  and  $\mathbf{T}\mathbf{c} \notin C_\alpha$ .

As each row of  $\mathbf{T}$  is equal to  $\pm \mathbf{e}_i^T$  and  $\mathbf{T}$  is full of rank, the row vectors of  $\mathbf{T}$  can be seen as a permutation of  $\mathbf{e}_0^T, \mathbf{e}_1^T, \dots, \mathbf{e}_n^T$ . The column vectors of  $\mathbf{T}$  are similar. So  $\mathbf{T}$  can be written as

$$(\pm \mathbf{e}_{i_1} \quad \pm \mathbf{e}_{i_2} \quad \dots \quad \pm \mathbf{e}_{i_n}) \quad (13)$$

where  $\mathbf{e}_{i_1}, \mathbf{e}_{i_2}, \dots, \mathbf{e}_{i_n}$  is a permutation of unit vectors  $\mathbf{e}_0, \mathbf{e}_1, \dots, \mathbf{e}_n$ .  $\square$

**Algorithm 5: Template Retrieve Attack on  $\mathbf{M} = \mathbf{TR}$** 

**Data:**  $\mathbf{M} = \mathbf{TR} \in O(n)$  with  $\mathbf{T} \in \mathcal{T}$  and  $\mathbf{R}$  is the native isometry rotation, threshold  $\theta_t, m$

**Result:**  $\mathbf{v}$  or  $\perp$

Create empty set  $V$

**for**  $k = 2, \dots, m$  **do**

**for**  $i' = 1, \dots, n$  // repeat  $n$  times

**do**

    Random select distinct  $k$  indices

$I = (i_1 < \dots < i_k \in [n])$

    Random select distinct  $k$  indices

$J = (j_1 < \dots < j_k \in [n])$

    Select the submatrix  $\mathbf{M}'$  of  $\mathbf{M}$  with row indices  $I$  and column indices  $J$

    Compute the null vector  $\mathbf{u} = (u_1, \dots, u_k)^T$  of submatrix  $\mathbf{M}'$

    Compute  $\mathbf{v} = (v_1, \dots, v_n)^T$  such that

$v_{j_i} = u_i, \forall j_i \in J$  and  $v_j = 0, \forall j \notin J$

**if**  $\mathbf{M}\mathbf{v}$  contains exactly  $i$  non-zero positions // make  $\mathbf{v}$  satisfy  $\mathbf{R}\mathbf{v} = \mathbf{v}$

**then**

      Store  $\mathbf{v}$  in  $V$

$\mathbf{M}' \leftarrow$  vertical stack of vectors in  $V$

$V' \leftarrow$  approximate null vectors of  $\mathbf{M}'$

**for**  $\mathbf{v} \in V'$  **do**

$\mathbf{c}' \leftarrow \text{Decode}(\mathbf{M}\mathbf{v})$

**if**  $\text{Angle}(\mathbf{M}\mathbf{v}, \mathbf{c}') < \theta_t$  **then**

    Output  $\mathbf{v}$

Output  $\perp$

Then we recall the naive isometry rotation defined in [24].

*Definition B.1 (naive isometry rotation).* Given vectors  $\mathbf{t}, \mathbf{c} \in \mathbb{R}^n$ , let  $\mathbf{w} = \mathbf{c} - \mathbf{t}^T \mathbf{c} \mathbf{t}$  and  $\mathbf{R}_\theta = \begin{pmatrix} \cos \theta & -\sin \theta \\ \sin \theta & \cos \theta \end{pmatrix}$  where  $\theta = \text{Angle}(\mathbf{t}, \mathbf{c})$ . The naive rotation matrix  $\mathbf{R}$  mapping from  $\mathbf{t}$  to  $\mathbf{c}$  is:

$$\mathbf{R} = \mathbf{I} - \mathbf{t}\mathbf{t}^T - \mathbf{w}\mathbf{w}^T + (\mathbf{t} \ \mathbf{w}) \mathbf{R}_\theta (\mathbf{t} \ \mathbf{w})^T \quad (14)$$

where  $\mathbf{I}$  is identity matrix.

The naive isometry rotation  $\mathbf{R}$  can be seen as rotating  $\mathbf{t}$  to  $\mathbf{c}$  in the 2D plane  $P$  extended by  $\mathbf{t}$  and  $\mathbf{c}$ . Therefore, there are vectors in  $(n-2)$  dimension subspace orthogonal to  $P$  that satisfy  $\mathbf{R}\mathbf{v} = \mathbf{v}$ . Restrict that  $\mathbf{v}$  only has few non-zero positions, we have  $\mathbf{TR}\mathbf{v} = \mathbf{T}\mathbf{v}$  filled with lots of 0s. By guessing the non-zero positions in  $\mathbf{v}$  and zero positions in  $\mathbf{TR}\mathbf{v}$ , we can calculate and filter to get  $\mathbf{v}$ . We can calculate the null space  $P'$  of  $\mathbf{M}'$  made of these vectors. As  $\mathbf{v} \perp P$ , with enough vectors, we can greatly shrink the space  $P'$  to  $P$  and finally retrieve  $P$ . If  $\mathbf{t}$  is the biometric template and  $\mathbf{c} \in C_\alpha$ , it's easy to retrieve  $\mathbf{t}$  knowing plane  $P$ .

However, by experiments, we find that the first null vector  $\mathbf{v}'$  of  $\mathbf{M}'$  is close enough to biometric template  $\mathbf{t}$ . Hence, we just take  $\mathbf{v}'$  as possible candidate and use the sketch algorithm to try to retrieve original template  $\mathbf{t}$  or  $-\mathbf{t}$ . The details are shown in Algorithm 5.

With  $n = 512, \alpha = 16$ , Algorithm 5 can output original template  $\mathbf{w}$  or  $-\mathbf{w}$  with probability  $\approx 60\%$  on 200 tests by setting  $m = 8$  and  $\theta_t = 30^\circ$ .